A Comprehensive Genetic Linkage Map of the Human Genome

NIH/CEPH Collaborative Mapping Group*

A genetic linkage map of the human genome was constructed that consists of 1416 loci, including 279 genes and expressed sequences. The loci are represented by 1676 polymorphic systems genotyped with the CEPH reference pedigree resource. A total of 339 microsatellite repeat markers assayed by PCR are contained within the map, and of the 351 markers with heterozygosities of at least 70%, 205 are microsatellites. Seven telomere loci define physical and genetic endpoints for 2q, 4p, 7q, 8p, 14q, 16p, and 16q, and in other cases distal markers on the maps have been localized to terminal cytogenetic bands. Therefore, at least 92% of the autosomal length of the genome and 95% of the X chromosome is estimated to be spanned by the map. Since the maps have relatively high marker density and numerous highly informative loci, they can be used to map disease phenotypes, even for those with limited pedigree resources. The baseline map provides a foundation for achieving continuity of clone-based physical maps and for the development of a truly integrated physical, genetic, and cytogenetic map of the human.

Genetic linkage mapping has become an important technology applied to the study of human biology and, in particular, for the delineation of the molecular basis of disease through gene isolation and characterization of mutations in DNA. Once the chromosomal location of a disease-producing gene has been determined, fine structure genetic mapping narrows the region to be searched. Subsequent studies often include examination of known genes mapping to the area and isolation of new genes by positional cloning strategies. The success of this approach has been stunning, and the pace is accelerating rapidly, due in large part to the availability of sets of mapped genetic markers and improvements in physical mapping methods. Landmarks from the past few years include isolation of genes responsible for cystic fibrosis (*1*), neurofibromatosis (*2*), and fragile X–linked mental retardation (*3*). Since these disorders segregate as single Mendelian traits and because reasonably large pedigree resources were available, there was every expectation that the genes eventually would be cloned and that the molecular basis of the disorders would be determined quickly. This prediction has been fulfilled. It was not obvious, however, that the bases for common disorders such as diabetes, colon cancer, breast cancer, and affective disorders could be resolved by this approach since they could be caused by multiple, independent genes and, in addition, might be influenced by environmental factors. Although progress in mapping bipolar affective disorder and schizophrenia has been slow (*4*), evidence supporting the feasibility of this approach for common diseases has come from reports of the isolation of a gene responsible for colon cancer (*5*); mapping of a breast cancer locus (*6*); and verification, by linkage and mutation analysis, that a candidate gene (glucokinase) is responsible for a form of diabetes (*7*).

Despite these successes, genetic linkage maps for the human chromosomes are not yet ideal for trait mapping. For example, the correspondence between the end points of the genetic linkage maps and the physical termini of chromosomes remains uncertain because only a few human telomeres have been identified in cloned DNA (*8–10*). Therefore, the extent to which the human genome is encompassed by genetic maps is not fully known. In addition, centromere-specific polymorphisms are available for only a few chromosomes, limiting the definition of these structures within the context of linkage maps. The most significant weakness of the currently available genetic maps, however, is the lack of highly informative markers that are evenly spaced along the chromosome. Most of the mapped markers are restriction fragment length polymorphisms (RFLPs) (*11*) assayed by DNA hybridization [see, for example, Donis-Keller *et al.* (*12*)]. Although these DNA markers are abundant in the genome, the most informative members of this class, VNTRs (variable number of tandem repeats) or minisatellites (*13*), tend to cluster near the ends of chromosomes (*14, 15*). Furthermore, only a small number of cloned genes have been incorporated into linkage maps because of the low degree of restriction site polymorphism within or nearby these coding sequences.

In addition to their utility for disease gene localization, genetic linkage maps could prove valuable for clone-based physical mapping of whole chromosomes, particularly as a means of facilitating closure attempts, since the position of contigs along the chromosome and locations of gaps could be readily identified. Until quite recently, the advantage of applying genetic mapping to this purpose and its use in focusing DNA sequencing efforts have not been fully appreciated because of the lack of high-resolution maps containing markers that could also be readily used as physical mapping reagents.

Because of the perceived need to quickly and systematically develop a high-resolution genetic linkage map of the human genome, several international efforts have been launched during the past several years. At the National Institutes of Health (NIH), the National Center for Human and Genome Research (NCHGR) initiated a program to develop "index maps" for each of the human chromosomes consisting of genetic markers with interval spacing of no more than 15 cM (centimorgans) and marker heterozygosity of at least 70% (*16*). Similar efforts to improve the existing genetic maps are also under way under the auspices of the European Genetic Linkage Map Project (EUROGEM) and Genethon (*17*).

These efforts have been greatly facilitated by the recognition that polymorphisms originating from microsatellite repeat elements, abundant and ubiquitous throughout the genome, could be exploited for genetic mapping if they were assayed by the polymerase chain reaction (PCR) and DNA sequencing gels (*18*). A relatively large number of these markers have already been developed (*19*). Furthermore, microsatellite markers have proven to be highly informative and well distributed throughout the genome. The presence of these markers in regions adjacent to coding sequences has enabled the incorporation of cloned genes into genetic linkage maps (*20*). The markers are also "ready-made" sequence tagged

*Correspondence should be directed to Dr. Mark Guyer, NIH, NCHGR, Building. 38A, Room 605, Bethesda, MD 20892, USA, or Dr. Howard Cann, CEPH, 27 rue Juliette Dodu, 75010 Paris, France. Maps of the individual chromosomes were constructed by the authors indicated with the map descriptions. Dr. Helen Donis-Keller served as coordinating editor for the assemblage of this work (Divison of Human Molecular Genetics, Department of Surgery, Washington University School of Medicine, St. Louis, MO 63110 U.S.A.)

sites (STSs), providing useful reagents for physical mapping (*21*).

Another important aspect in the development of genetic maps was, and continues to be, the availability of a common reference pedigree collection and a shared genotype repository. The Centre d'Étude du Polymorphisme Humain (CEPH), established in 1984 by Jean Dausset and Daniel Cohen, provides DNA from a set of reference pedigrees to collaborating laboratories (currently 99 worldwide), maintains a genotype database that is distributed regularly, and sponsors the construction of consortium linkage maps (*22*).

Finally, the development of statistical methods embodied in computer programs (*23–26*) have made possible construction of high-resolution genetic maps containing 100 or more markers. In addition, the availability of high-speed and relatively inexpensive workstations for linkage calculations has made this type of research accessible to a large number of laboratories.

Map-making has been transformed over the past 10 years from a relatively arcane pursuit by a small number of human genetics groups to an intensive, highly collaborative process, often involving many laboratories. This activity has led to the publication of many independent maps presented in a variety of formats. Therefore, it is not possible to readily achieve a "view" of the entire genome. Such a "view" is crucial for those interested in designing efficient strategies for screening the human genome in search of locations for heritable traits. It also has become apparent that defining chromosome deletions by means of mapped genetic markers is quite useful for pinpointing the locations of putative tumor suppressor genes implicated in a wide variety of neoplasias [for example, see (*27, 28*)].

To unify a large amount of genotypic data currently available from the CEPH database and collaborating laboratories, members of the genetic mapping community have joined together to construct a genetic linkage map of the human genome which is presented here in a common format. The map should provide a useful tool for disease gene mapping, for defining chromosome deletions, and for assessing current progress and future directions for human genetic linkage mapping.

Results

Genetic markers and genotypic data. Characteristics of the 1676 genetic markers used to construct the genetic maps reported in this study are summarized in Table 1 (see Appendix, pages 148 to 159). Cytogenetic band assignments for markers that have been physically mapped are indicated along with the relevant literature citations (a subset of these assignments is also shown in Fig. 1). The markers are grouped by chromosome and listed alphabetically according to locus name within each grouping. Markers that have not been assigned gene abbreviations or D segment numbers are placed at the end of the relevant chromosome listing. Unless otherwise indicated, the informativeness [heterozygosity and polymorphism information content (PIC)] for the markers has been calculated from the genotypes used to construct the maps.

Genotypic data consisted of RFLPs assayed by Southern blot hybridization (1317 systems), protein polymorphisms (17 systems, assayed by a variety of methods including gel electrophoresis, serologic testing, and enzymatic assay), single base change polymorphisms assayed by the oligonucleotide ligation assay (OLA) (three systems; see chromosome 14), and microsatellite polymorphisms assayed by PCR (339). These data are available to interested investigators (*29*).

Error checking of genotype data was routinely performed prior to map construction. For example, the inheritance of polymorphic alleles in families was tested for parental exclusions (an indicator that individuals in the pedigree have been mislabeled or that genotypes have been incorrectly scored). The chromosome 1 genotype data underwent multiple checks during the building process for the CEPH consortium map, as discussed in Dracopoli *et al.* (*30*), as did much of the data used in additional map construction projects of the CEPH consortium (*31*). All groups (with the exception of those working on chromosomes 11 and 18) checked the CEPH V5 data for errors, usually through examining the CRI-MAP CHROMPIC output (*25*) for apparent close double crossovers and intralocus recombinants. Nearly all laboratories retyped suspect data from microsatellite markers (most of which were found as apparent double recombinants). Although no error checking was performed on the CEPH database for chromosome 18, after it was merged with new data, all suspect data were regenotyped and corrected before the final map was produced. Few laboratories retyped RFLP markers, but when autoradiographs were accessible, questionable data were reexamined; for example, all the CRI-RFLP markers on chromosome 20 were rescored. For chromosomes 4 and 15 suspect data were not removed from the data set during the map construction process. Changes to genotypes in systems from chromosomes 18 and 19 were done only after regenotyping.

We found several markers in the CEPH database chromosome files that genetically map to a chromosome other than the one from which they were thought to originate. Incorrect placement of a marker on a chromosome was suspected when, in multipoint map runs, a marker could not be placed uniquely and the mapping program would choose the best (nonunique) placement at either end of the chromosome, or place it in most map intervals over the entire map length. These markers were tested against the entire CEPH V5 database in two-point linkage analyses and multiple, significant (>LOD 4.0) linkages with markers from other chromosomes revealed their true origins.

Methodologies used for construction of the linkage maps. Several computer program packages are currently available for the construction of human multipoint linkage maps. One of the first program packages of this type to be described, LINKAGE (*23*), was used [with a modified version of CILINK, (*32*)] to construct genetic maps described in this report for chromosomes 5 and 17. In addition, the maps for chromosomes 5 and 17 were built with an automated iterative algorithm (*32–34*) that utilizes a primary ("skeleton") map and adds unmapped loci to the map after performing multi-point analyses. In a single iteration, however, only one marker can be added to any interval, and none to intervals adjacent to intervals receiving new markers. At each step, a new skeleton map is generated and validated, and then the process is repeated until no additional markers can be added to the map. The final distances for the chromosome 1 map shown here were calculated with LINKAGE, with other independent multipoint map orders constructed with MAPMAKER [version 1.0 (*26*)] and CRI-MAP [version 2.4 (*24, 25*)] as described in Dracopoli *et al.* (*30*).

Fourteen chromosome maps were constructed by means of the program package CRI-MAP [version 2.4 (*24, 25*)] (chromosomes 2, 3, 6, 7, 8, 10, 11, 12, 13, 14, 15, 16, 20, and 21). Similarly, the chromosome 18 map was constructed by means of CRI-MAP and CILINK in combination. CRI-MAP and CROSSMAP (*35*), a new program that evaluates map order solely on the criterion of crossover minimization, were used to build the chromosome 19 map. The chromosome 4 and X maps were constructed with CRI-MAP (*25*) in conjunction with a previously described map-building strategy (*36*). The sequence followed with CRI-MAP, in general, is to use the BUILD option first to generate initial maps each beginning with two highly informative markers spaced approximately 10 cM apart (determined by initial two-point analyses). Markers are then uniquely assigned to this map if their placement in an interval is at least 1000:1 more likely than placement in the next best interval, and the most likely intervals for placement of the remaining (nonunique) markers are also determined.

The CHROMPIC option is used to identify the locations of likely data errors, and after correction of the data set, the process is repeated. After new BUILD analyses, the FLIPS option is used to test permutations of markers (commonly in sets of three or four) to identify the best map order. MAPMAKER [version 1.0 (26)] was used to construct the genetic map for chromosome 9. In the case of chromosome 22, both MAPMAKER and CRI-MAP were used for map construction.

For all maps, the criteria established for odds of marker order were at least 1000:1, regardless of the map construction programs or strategies chosen. Loci that were not ordered uniquely by these criteria were placed along the intervals to which they could reside (as shown in Fig. 1). In general, the various mapping programs produce maps with comparable genetic orders. Both CRI-MAP and MAPMAKER were written expressly for the purpose of quickly finding the best genetic order for large numbers of loci and they perform that task well. The major difference between CRI-MAP and MAPMAKER (from the user's perspective) is that CRI-MAP takes advantage of more genotypic data, inferring genotypes where possible. Because LINKAGE, which has traditionally been used for disease mapping, uses more of the genotypic data set in its calculations, it produces more accurate recombination fractions but is slower and not practical for the simultaneous mapping of large numbers of markers. Statistical support for map order is termed local (odds for inversion of small sets of markers) or global (support for one entire map order over another map order). Local support is less robust and is very sensitive to genotyping errors.

The genetic maps. Graphical representations of the chromosome maps, which include a total of 1416 genetic loci, are given in Fig. 1. For each chromosome, one linkage map is shown representing the sex-average map for which recombination between the sexes was not distinguished. Also shown are idiograms representing the banding pattern of metaphase chromosomes stained with Giemsa dye and observed under the light microscope (*37*). A subset of genetic markers on the sex-average map sublocalized by physical methods, such as fluorescence in situ hybridization (FISH), are connected to their chromosomal band assignments in the idiogram. These genetic loci served to orient the linkage maps and assisted in estimating the extent of genetic and physical chromosome coverage. Recombination frequencies for all maps have been converted to centiMorgans by means of the Kosambi mapping function.

Table 2 summarizes the predicted and observed genetic map distances for each of the chromosomes. Also included are the estimates for the physical lengths of the chromosomes (*38*) and the percent of the physical distance included in the genetic maps. For chromosomes 1 to 16 and chromosome 22, the observed sex-average length exceeded the predicted length based on chiasma counts, except for chromosomes 12 and 16 which are within 2% and 10% of the chiasma estimate, respectively. For chromosomes 17 to 21, the observed lengths of the sex-average maps were somewhat less than the chiasma estimates. However, in all cases the genetic distance (in centimorgans) exceeded the estimated physical distance (in megabases), if one assumes a correspondence of 1 cM = 1 Mb. Maps of the individual chromosomes were constructed by the authors indicated with the map descriptions; their affiliations are listed at the end of the References and Notes section.

Table 2. Predicted and observed map lengths. Estimates for the physical lengths of the chromosomes and mean chiasma map lengths were taken from N. E. Morton (*38*). In some cases, estimates of the physical lengths of the chromosomes contained within the genetic maps were based on genetic markers developed from cloned telomere segments (chromosomes 2, 4, 7, 8, and 14) or by physical mapping that established the subtelomere locations of genetic markers to within a few hundred kilobases of the T_2AG_3 telomere repeat element (chromosome 16, p and q). For other cases, estimates were inferred from cytogenetic localizations of markers from the most distal portions of the linkage maps and by estimating the percentage of the chromosome arm included within these cytogenetic bands. For example, in the case of chromosome 8, an 8p telomere polymorphism estimated to reside within 150 kb of the T_2AG_3 repeat defines the physical and genetic end point of the short arm of the chromosome. The penultimate marker from the 8q linkage map and uniquely localized (D8S139) maps to the most terminal cytogenetic band (8q24.3–qter), which we estimate spans approximately 5% of the long arm. In addition, the terminal uniquely localized 8q genetic marker, *GPT*, extends the linkage map approximately 19 cM in the distal direction. Therefore, from these observations we estimate that the genetic map covers approximately 95% of 8q and 100% of 8p.

Chr.	Predicted physical length (Mb)	Chiasma (mean cM)	Observed lengths (cM)			Estimated physical map coverage		Mapped telomere
			Male	Female	Sex avg	%p	%q	
1	263	282	308	478	390	95	95	—
2	255	261	283	442	354	95	100	q
3	214	188	276	399	334	95	95	—
4	203	231	208	356	275	100	95	p
5	194	198	245	363	297	95	95	—
6	183	213	194	321	249	90	98	—
7	171	178	207	355	267	95	100	q
8	155	172	183	298	237	100	95	p
9	145	146	128	220	170	70	95	—
10	144	167	191	322	250	95	95	—
11	144	150	225	276	245	95	95	—
12	143	196	144	289	201	90	90	—
13	114	130	193	246	219	0	95	—
14	109	113	134	216	171	0	95	q
15	106	148	146	212	178	0	95	—
16	98	145	133	197	162	99	98	p, q
17	92	196	137	200	168	95	95	—
18	85	143	72	161	109	70	90	—
19	63	146	98	134	114	85	80	—
20	72	180	135	162	147	95	95	—
21	50	70	57	78	67	0	95	—
22	60	81	81	115	98	0	90	—
X	164	NA	NA	208	NA	95	95	—

Chromosome 1

N. C. Dracopoli[a], P. O'Connell[b], T. I. Elsner[c], J.-M. Lalouel[c], R. L. White[c], K. H. Buetow[d], D. Y. Nishimura[e], J. C. Murray[e], C. Helms[f], S. K. Mishra[f], H. Donis-Keller[f], J. M. Hall[g], M. K. Lee[g], M.-C. King[g], J. Attwood[h], N. E. Morton[i], E. B. Robson[h], M. Mahtani[j], H. F. Willard[j], N. J. Royle[k], I. Patel[k], A. J. Jeffreys[k], V. Verga[l], T. Jenkins[l], J. L. Weber[m], A. L. Mitchell[n], A. E. Bale[n]

This map is a reproduction of the CEPH consortium linkage map of human chromosome 1 (*30*). The map contains 99 loci [128 systems; see (*16*) for a discussion of systems]. Fifty-eight loci are uniquely placed on the map with likelihood support >1000:1, and the remaining loci that are not excluded with these odds are arrayed in narrow intervals along this fixed map. D1Z2 and D1S68, located in the terminal bands of both chromosome arms, also define the

genetic end points. Therefore we estimate that the linkage map reflects approximately 95% of the physical length (263 Mb) (38) of the chromosome. The map is anchored at the centromere by the uniquely placed α-satellite polymorphism, D1Z5. The male, female, and sex-average maps extend for 308, 478, and 390 cM, respectively. Comparison of 4205 genotypes submitted in duplicate demonstrated a typing error rate of 0.6%. Therefore, the length of these multipoint maps is likely to be inflated by approximately 68 cM. Although RFLP markers currently dominate the map (only six microsatellite repeats are included), genotypes from a recently constructed chromosome 1 microsatellite map of 33 loci (39) will be available for development of a detailed combined map in the future.

Chromosome 2

R. Anker[a], T. Steinbrueck[a], M. Holt[a], J. L. Weber[b], H. Donis-Keller[a]

The sex-average linkage map for chromosome 2 is 354 cM in length: 283 cM for males, 442 cM for females. Although this is considerably longer than the estimate (261 cM) based on chiasma counts (38), the observed length is consistent with genetic measurements for chromosome 1 (which is very close in physical length to chromosome 2) and similar with respect to the number of mapped markers. We estimate that more than 95% of the physical length of chromosome 2 (255 Mb) (38) is contained within the genetic map since one of the most distal markers on the short arm, ACP1, has been cytogenetically mapped to 2p25–pter, and the q terminus is contained within a telomere YAC clone (8), D2F69S1, that detects three RFLPs. The same cosmid subclone that detects the 2qter polymorphism (with LODs of 12 to 73 with multiple markers) detects two RFLP systems at the p terminus of chromosome 8 (see chromosome 8 description). Altogether there are 22 mapped markers with heterozygosities of at least 70%; 10 are RFLPs and 12 (from a total of 21) are microsatellite polymorphisms. A total of 79 loci (96 systems) are included in the map and 36 have been uniquely localized. The sex-average map contains seven intervals that exceed 15 cM, and one of these near the p terminus constitutes a genetic gap of nearly 60 cM. Our map is similar in length and number of uniquely localized markers to the recently reported CEPH consortium map (40) except that the CEPH map included a single microsatellite marker (ours has 21) and we have added 24 new polymorphic systems including a telomere locus.

Chromosome 3

S. L. Naylor[a], S. Sherman[b], H. A. Drabkin[c], E. Whishenand[c], D. Garcia[a], R. Chinn[a], B. DuBois[a], P. Wilkie[d], J. L. Weber[d], Y. Nakamura[e]

The sex-average map spans 334 cM and consists of 51 loci, of which 48 have been uniquely placed. Although neither telomere has yet been cloned, we estimate that approximately 95% of the physical length of the chromosome is included in the genetic map on the basis of correlations between distal linkage markers that have also been placed within the cytogenetic map. The average interval between markers is about 7 cM although there are some gaps occurring in the telomeric regions. However, no gap is greater than 20 cM on the sex-average map. The sex-specific maps are 276 cM and 399 cM for males and females, respectively. For some intervals, there is significantly more recombination occurring in males compared to females. Seventeen microsatellite markers have been incorporated in the map, and of the 13 markers with heterozygosities in excess of 70%, 11 are microsatellites that are relatively evenly distributed along the length of the map.

Chromosome 4

J. C. Murray[a], K. H. Buetow[b], T. Hudson[c], J. L. Weber[d], T. Scherpbier-Heddema[b]

The sex-average map length of this framework map is identical to the 39-locus map reported by Mills *et al.* (36). However, the male map is 10 cM shorter and the female map 9 cM longer than the Mills *et al.* map (36). Ten of the 81 markers reported in this map have heterozygosities of at least 70%, and six of these are microsatellite markers (from a total of 25) assayed by PCR. The largest gaps in the map are 26 cM in the female map and 18 cM in both the sex-average and the male maps. In the sex-average map, the average interval distance is 7 cM, with 28 of the 38 intervals being less than 10 cM. Differences in position-specific recombination rates for the chromosome 4 linkage map have been recently described (41). Except for the most distal portions of the map that are represented by highly informative RFLPs, the current map contains highly informative microsatellite markers that are relatively evenly spaced. In addition, since there are currently no gaps greater than 20 cM on the sex-average map, the map reported here provides a useful framework against which to carry out linkage studies.

Chromosome 5

R. Plaetke[a,b], L. Bernard[c], M. Carlson[b], A. J. Jeffreys[d], Y. Nakamura[e], A. E. Retief[f], L. Warnich[f], B. Weiffenbach[g], S. Wood[c], R. L. White[a, h]

The map was built with markers from more than 200 available for chromosome 5 in the CEPH database (V5). Except for one marker, D5S71, which has a heterozygosity of 31%, selection of markers was based on heterozygosities of at least 40%, and on children (more than 100) from matings where at least one parent is heterozygous. We constructed the map with the program package LINKAGE (23) and an automated algorithm (34) that adds "test markers" to a primary map after evaluating their location with multipoint analysis. The 20-marker primary map (loci marked "•" in Fig. 1) was validated, and odds against inversion of adjacent loci were greater than 1000:1 in every case. Of the 42 markers in the final map, 41 are RFLPs. Four markers have heterozygosities of at least 70%, and four others have heterozygosities ranging from 67 to 70%. Numerous microsatellite markers are now available and it is expected that chromosome 5 will soon be represented with a map that contains highly informative markers assayed by PCR. All but four pairs of loci map with odds of at least 1000:1 against local inversion. The loci at four intervals can be permuted and the appearance of the markers in the order shown in the map represents the most likely as follows: D5S48–D5S73 (35:1), D5S56–D5S59 (282:1), D5S39–*HEXB* (67:1), D5S390–D5S64 (279:1). At 297 cM, the sex-average map is slightly longer than the map published by Weiffenbach *et al.* (42). Physical mapping data allowed us to locate the centromere between *HPRTP2* and D5S76; more precise localization was not possible because we were able to map D5S21 only within a 1-LOD unit confidence interval. The order of markers on our map agrees with two published maps (42, 43); on a third, however (44), the order of D5S83 and D5S71 was reversed, with odds of 10:1. When the location of D5S83 on our map was determined by including the information of three adjacent loci on each side, the odds against inversion with D5S71 were 13360:1.

Chromosome 6

M. Chen[a], S. K. Mishra[a], H. Y. Zoghbi[b], R. Cottingham[b], H. T. Orr[c], H. M. Cann[d], H. Donis-Keller[a]

The genetic map was constructed from 61 loci (77 polymorphic systems) with 38 loci uniquely placed along a sex-average length of 249 cM. Fourteen systems (12 loci) have heterozygosities of at least 70%, and four of these are microsatellites assayed by PCR. The major histocompatibility complex (*MHC*) at 6p21.3 constitutes one of the most dense regions of expressed

sequences in the human genome, with over 70 functional genes that map within it. In addition to the *MHC* complex genes, 21 other genes and transcribed sequences are contained within this map. Several loci responsible for inherited disorders have been mapped to chromosome 6, including a gene for one form of spinocerebellar ataxia (*SCA1*) which is very closely linked to D6S89 at 6p23 (*45*), and a gene for retinitis pigmentosa (*RP6*) mapped to the short arm of chromosome 6, centromeric to the *HLA* loci (*46*). Furthermore, mutations in a gene which maps to this region, peripherin-RDS, a photoreceptor cell-specific glycoprotein, have been shown to cause this form of *RP* (*47*). Since neither telomere has been mapped, evidence that most of the physical length of the chromosome [183 Mb; (*38*)] is contained within the genetic map is based only on cytogenetic assignment of the genetic markers near the ends of the map to specific cytogenetic bands. For example, a cluster of 11 markers map within 6q27, the most terminal cytogenetic band on the long arm. At the p terminus the F13A1 locus, 17.4 cM proximal to D6S7, maps to 6p24–pter (*48*). The estimated genetic length (213 cM), based on chiasma counts (*38*), is 85% of the observed genetic length of the sex-average map; however, the map reported here has several intervals, particularly on the long arm, with significant genetic gaps. The most underrepresented region lies between D6S26 and *TCP1*, which contains only three loci uniquely placed within a region of nearly 90 cM on the sex-average map. The female map (321 cM) is approximately 65% larger than the male map (194 cM), and for nine intervals we observed statistically significant sex-specific recombination differences.

Chromosome 7

C. Helms[a], S. K. Mishra[a], A. K. Burgess[a], S. L. Cline[a], D. Knobloch[a], A. V. Hing[a], G. Vergnaud[b], H. Donis-Keller[a]

The chromosome 7 baseline map contains 112 loci, with 52 loci uniquely placed, including markers physically localized to the p terminal band and several 7q telomere markers. Because of the relatively low number of informative meioses, the centromere locus D7Z2 is not uniquely placed at 1000:1 odds, and maps instead to five genetic intervals spanning 18 cM on the sex-average map. The sex-average map length is 267 cM, the female map is 355 cM, and the male map is 207 cM. We estimate that the map covers at least 97% of the chromosome. This map is 50% longer than the map length predicted on the basis of chiasma counts (*38*). The largest genetic gaps between uniquely placed loci are 21 cM in females (*ERV3*–D7S398) and 12.8 in males (D7S372–D7S396). The map has an overall sex-average intermarker distance of 2.36 cM and is one of the most densely mapped chromosomes in the human genome at the present time.

The genetic map order agrees well with previously described chromosome 7 maps (*48*). While the map is dominated by RFLPs, 13 microsatellites including three gene markers [*EGFR*, *COL1A2*, and *GCK* (*49*)] have now been incorporated. Of the 25 markers with heterozygosities of at least 70%, nine are microsatellites. A total of 13 genes are localized in this map, including the *TCRG* and *TCRB* gene clusters, and the cystic fibrosis locus (*CFTR*), which is known to lie near the highly informative locus D7S23 (*50*). The high concentration of genetic markers on the map will provide an excellent resource for mapping with high precision other chromosome 7 loci, such as those implicated in holoprosencephaly (*51*), breast cancer (*27*), and split hand and foot syndromes (*SHFD*) (*52*), in addition to its usefulness for whole genome screens for disorders which are as yet unmapped.

Chromosome 8

T. Steinbrueck[a], C. Read[a], S. P. Daiger[b], L. A. Sadler[b], J. L. Weber[c], S. Wood[d], H. Donis-Keller[a]

The sex-average genetic linkage map spans 237 cM and includes 59 loci (79 systems), 40 of which are uniquely placed. Of the 23 microsatellite markers contained within the map, 13 have heterozygosities of at least 70%. Microsatellite markers have not yet been mapped to the most distal one-third of the long arm; however, D8S28 (one of the two RFLPs with heterozygosities greater than 70%) provides an informative locus in this region. A telomere marker D8F69S2, identified from a YAC telomere clone, sets the physical and genetic boundary for the 8p terminus (*8*, *53*). In addition, different allele systems detected by the same telomere probe map to 2qter (see chromosome 2 description). The extent of coverage is less certain for the long arm because the most distal marker, *GPT*, could lie at any point along the interval q24.2–qter. As this band is roughly 5% of the chromosome, we estimate that the genetic map includes approximately 95% of the physical length (155 Mb) (*38*). Consistent with other observations for human chromosomes, we find that the female map length (298 cM) is roughly 1.5 times the length found for males (183 cM). The map reported here includes genotypic data from 22 loci used to construct a recently reported map (*54*). The order of markers shared in common is identical except for an inversion between D8S171 and D8S131. However, our map is 30 cM larger for the interval spanned and contains an additional eight markers uniquely mapped within this interval. We confirm that the most distal marker on the p arm from Tomfohrde *et al.* (*54*) is very near the telomere, since it maps 3.3 cM proximal to D8F69S2. Several important disease loci have been mapped to chromosome 8 recently, including a gene for one form of retinitis pigmentosa (*RP1*) mapped to the pericentromeric region near *PLAT* (*55*), and Werner's syndrome, a recessive trait with the appearance of accelerated aging that has been mapped to an interval on 8p between D8S87 and *ANK1* (*56*).

Chromosome 9

D. J. Kwiatkowski[a], S. Povey[b], J. Armour[c], J. Attwood[b], R. A. Furlong[d], D. R. Goudie[d], J. L. Haines[e], M. A. Pericak-Vance[f], S. Slaugenhaupt[e], G. Vergnaud[g], L. Warnich[h], M. A. R. Yuille[d]

The map of chromosome 9 consists of 32 uniquely ordered markers and an additional 25 markers mapped to more than one interval. Twenty-one of the markers have heterozygosities greater than 70%. Twenty-four can be assayed by PCR, 30 by Southern blot, and three by analysis of protein polymorphisms. The map has a sex-average length of 170 cM, with female length 220 cM and male length 128 cM, reflecting increased recombination in females in all regions apart from 9q34–qter. Comparison with published maps (*12*, *57*) shows good concordance apart from the D9S58–D9S60 interval, which is significantly expanded in the current map, possibly due to errors. The largest gap in the map is on 9p between D9S54 and *IFNB1* (26.6 cM). Because the telomere has yet to be cloned and the most distal marker, D9S54, is broadly localized on the cytogenetic map to 9p22–pter, an interval of unknown genetic distance remains to be incorporated at 9pter. However, we expect that the 9q map covers nearly all of 9q since several markers are found in the distal band, 9q34. We observed suppressed recombination in the pericentromeric region, and increased recombination in both subtelomeric regions.

Chromosome 10

T. P. Keith[a], K. Falls[a], H. M. Cann[b], J. L. Weber[c], G. Vergnaud[d], C. Zheng[a], P. Phipps[a], K. Serino[a], J. Mao[a]

The map of chromosome 10 was constructed with 111 polymorphic systems (89 loci) from the CEPH V5 database (*58*), and 13 new microsatellite markers, genotyped by PCR. Fourteen markers have heterozygosities of at least 70%, and seven of these are microsatellites. The map contains 42

ordered loci with global support of 1000:1 odds and local support of at least 1000:1 where the log of the relative odds for placement, by the permutation of adjacent trios, was 3 or greater. The male map spans 191 cM and the female map spans 321 cM. No interval on the sex-average map exceeds 20 cM. The largest distance between two adjacent markers is 12 cM for D10S33–D10S32 on the male map and 30 cM for *VIM*–D10S89 on the female map. Two-point LOD scores for each map interval show a statistically significant ($P < 0.05$) excess of recombination in males for the intervals D10S33–D10S32, pCMM14–D10S180, and D10S180–D10S112 and an excess in females for the intervals D10S17–D10S28 and D10S62–D10S4. The linkage map extends to approximately 95% of the physical length (144 Mb) (*38*), and while the centromere-specific polymorphic marker D10Z1 has not been incorporated into the map, markers on each side of the centromere (for example, D10S34 and D10S11) identify this region. In addition, two new highly informative microsatellite markers that closely flank the centromere have recently been reported (*59*) and should further refine the pericentromeric region. Thirty-seven markers included in this map were previously used to develop the CEPH chromosome 10 consortium map (*31*), and this reported order was also used as a reference to confirm our map order. Twenty of the 28 loci from the CEPH consortium map were placed on the present map, and the orders were consistent between the maps.

Chromosome 11

P. Kramer[a,b], W. Becker[a], P. Heutink[c], M. James[d], C. Julier[d], M. Lathrop[d], J. A. Luty[a], Z. Wang[c], J. L. Weber[c], P. Wilkie[c], M. Litt[a,e]

The map consists of 72 loci with 41 uniquely placed along a sex-average map length of 245 cM. Seventeen of the loci have heterozygosities of at least 70%, 69 are RFLP markers, and 12 are microsatellites assayed by PCR. There are no major inconsistencies between marker order in the current map and the orders presented in previous maps (*12, 60*). The largest gap between markers occurs at the terminus of the long arm, between D11S129 and D11S387 (19.3 cM on the sex-average map). Other gaps of substantial size occur in p13 between D11S151 and D11S467 (16.7 cM) and p15 between HBB and D11S419 (15.9 cM). The female map is 276 cM in length and the male map is 225 cM. In general, female distances are as much as two to three times greater than male distances in the central region of the chromosome. However, as one moves toward the telomeres, male and female distances tend to equalize somewhat; then, in the most distal region, male distances show a marked and significant increase over female distances. This pattern is especially notable on the long arm. In constructing this map, the CEPH database was used directly without attempting to identify and remove probable typing errors. This may account for the 1.5-fold increase in map length over that predicted from chiasmata counts (Table 2). It may also account for the discrepancy between the physical and genetic localizations of the marker D11Z1, which maps physically to the centromere and genetically distal to D11S429, a marker localized to 11q13.1 by FISH.

Chromosome 12

M. Holt[a], D. Rains[a], T. Steinbrueck[a], J. L. Weber[b], H. Donis-Keller[a]

The sex-average genetic linkage map for chromosome 12, which includes 54 loci (73 systems), is 201 cM in length. The female (289 cM) is twice the length of the male map (144 cM). The largest interval (23.5 cM) on the sex-average map is between 1RB2.3 and D12S60. The lack of markers mapping between markers *IGF1* and D12S60 may explain the large intervals in this region. Twelve of the 15 markers (13 loci) with heterozygosities of at least 70% are microsatellites. Of the 27 uniquely placed markers, 10 loci have a heterozygosity of at least 70%. Because the localizations of distal genetic markers on both ends of the maps to cytogenetic bands are fairly broad, we estimate that the genetic linkage map covers approximately 80% of chromosome 12. However, we have recently identified a polymorphism from a YAC telomere clone derived from chromosome 12 that is linked to the most distal markers on 12p including the *vWF* locus [two-point LODs range from 3.6 to 29 (*61*)] which should allow us to precisely define the distal portion of 12p in a multipoint map. A total of 16 genes have been mapped to chromosome 12, accounting for nearly one-third of the markers genetically mapped. There are a total of five markers at the *f8VWF* locus, and four of these are microsatellites.

Chromosome 13

A. M. Bowcock[a], S. L. Osborne-Lawrence[a], R. I. Barnes[a], C. Dunn[a], R. L. White[b], S. Gerken[b], G. Vergnaud[c], A. E. Retief[d]

The map contains 74 loci that span 193 cM in males and 246 cM in females. It is likely that at least 95% of chromosome 13q is mapped, since both a centromeric marker at D13Z1 and loci sublocalized to the most distal band of 13q have been incorporated. Four additional centromeric markers at D13Z1 [described by Jabs *et al.* (*62*)] exhibit substantial recombination between each other and were not placed uniquely on the map. Morton (*38*) has estimated that chromosome 13q spans 100 cM in males and 160 cM in females. Since our male map is nearly twice this length, we expect that such an inflation in map length may be due to undetected errors in the genotypic data.

With respect to previously published maps, Donis-Keller *et al.* (*12*) have described a map of chromosome 13 that contained 10 loci and spanned 50.1 cM in males and 79 cM in females; however, more than 40 cM was contributed to the length of the map by one locus (D13S3) separated from the linkage group. Leppert *et al.* (*63*) described a map that contained 16 loci and spanned a region between D13S6 and D13S3 that was 80 Mb in males and 243 Mb in females, and Bowcock *et al.* (*64*) constructed a map of chromosome 13 that contained 39 loci and spanned 172 cM in males and 209 cM in females. Twenty-six of the loci included in the Bowcock *et al.* (*64*) map are included in the current 1000:1 odds map. Thirty-six of the loci on this map are detected with Southern blotting and 11 are detected with PCR amplification (*65*). Twelve markers with more than 70% heterozygosity were used to construct this map.

The largest gap on the sex-average map is 12.6 cM and is between D13S127 and *TUBBP2*. The average distance between uniquely placed loci is 4.8 cM. The ratio of female-to-male recombination is 1.3:1. Five intervals with statistically significant sex differences were observed. Only one of these intervals (D13S1–D13S127) shows an excess of recombination in females ($\chi^2 = 6.12$, $P = 0.013$). An excess of recombination in males was observed near the distal end of the map between D13S49 and D13S54 ($\chi^2 = 6.81$, $P = 0.009$). The sublocalization of markers agrees with the genetic map except for *ATP1AL1*, which was mapped more distally with somatic cell hybrids (*66*), and D13S64, which was mapped to a more proximal location (*67*).

Chromosome 14

H. Donis-Keller[a], R. Weaver[a], S. Ramachandra[a], C. Warlick[a], A. K. Burgess[a], J. L. Weber[b], M. Litt[c], D. A. Nickerson[d], C. A. Boysen[d], L. Hood[d], S. K. Mishra[a]

This is the first map of chromosome 14 that is continuous along the length of the long arm; it is bounded at the q terminus by a highly informative polymorphic locus, D14S82, that was identified from a YAC telomere clone. No polymorphic markers have been mapped to the short arm of this acrocentric chromosome, and because of the absence of observed chiasma in male

meioses, there is no estimate for genetic length [for a physical distance of 16 Mb (*38*)]. The 14q sex-average genetic map is 171 cM. The female map is 216 cM in length, which is approximately 60% longer than the male map (134 cM). Eight intervals with statistically significant sex-specific recombination frequencies were observed, and in all cases female exceeded male recombination. Thirty loci, from a total of 42 (49 systems) that were used to construct the map, are uniquely placed. The markers, which include 15 loci with heterozygosities of at least 70%, are well distributed along the map with the largest interval for the sex-average map of 16.7 cM (D14S52–D14S42). In addition to 13 microsatellite markers, three site polymorphisms assayed by the oligonucleotide ligation assay [OLA (*68*)] are included in the map.

Genotypic data used to construct the recently reported nine-microsatellite marker map (*69*) have been incorporated into the map reported here. The Wang and Weber map is contained within the interval D14S50–D14S51 on our map (the order of shared markers is identical), and our map extends the chromosome 14q map by 51.5 cM in the telomere direction and 14.5 cM towards the centromere. Seven genes or expressed sequences have now been mapped to 14q including the β-myosin heavy chain gene which has been shown to be responsible for a form of familial hypertrophic cardiomyopathy previously mapped to 14q11 (*70*).

Chromosome 15

A. M. Bowcock[a], R. I. Barnes[a], L. E. Weiss[a], J. Tomfohrde[a], N. C. Dracopoli[b], T. Hudson[b], M. Sarfarazi[c], P. Tsipouras[c], T. Jenkins[d], G. Vergnaud[e]

The map contains 53 loci that extend from 15q11.2-q12 in the Prader-Willi/Angelman syndrome region (*AS/PWS*) to 15q25-qter. The map spans 146 cM in males and 212 cM in females and therefore has a female-to-male recombination ratio of 1.5:1. A previously published map of chromosome 15 (*71*) contained 16 loci and spanned 146 cM in males and 187 cM in females. Ten of the loci used in this map are contained in our 1000:1 odds map. Donis-Keller *et al.* (*12*) described a map with nine linked loci, five of which are contained in this baseline map. A CEPH consortium linkage map of chromosome 15 has recently been described (*72*) and contains 19 of the RFLP-based markers and 5 of the PCR-based markers included in this map. The order of loci in previous maps does not conflict with that shown here. Thirty-nine of the markers used to construct the baseline map are RFLPs, and 18 are detected with PCR. There are 13 markers on the 1000:1 odds map with a heterozygosity of at least 70%. Nine of these are PCR-based. The largest gap on the map is 14.2 cM and is between D15S74 and D15S107. The average distance between uniquely placed loci is 6.1 cM and the on-average spacing is 4.8 cM. Six intervals with statistically significant sex differences were observed. Four intervals show an excess of recombination in males (for example, D15S29/D15S38–D15S36, $\chi^2 = 9.29$, $P = 0.002$). The most proximal region showing an excess of recombination in females is between D15S97 and *GABRB3* in the *AS/PWS* region ($\chi^2 = 5.89$, $P = 0.015$). The last interval shows an excess of recombination in males and is located between D15S87 and D15S3 at the distal end of the map ($\chi^2 = 14.21$, $P = 0.0002$). An excess of recombination in males at the distal ends of some of the autosomes has been reported previously (*15*).

The genes for Marfan syndrome (*MFS*) and the recessive form of limb-girdle muscular dystrophy (*LGMD2*) have been mapped to chromosome 15, at or near *FBN1*. This study identified several microsatellite markers, including two tetranucleotide repeats (MH22 and CYP19), and one $(CA)_n$ dinucleotide repeat (D15S103) that are closely linked to *FBN1*. In addition, a $(CA)_n$ dinucleotide repeat marker, D15S97, was mapped between D15S11 and *GABRB3* within the vicinity of the *PWS/AS* region.

Chromosome 16

H. M. Kozman, G. R. Sutherland, J. C. Mulley

The current genetic map is based on 67 polymorphisms from 50 loci. These have been placed into one of the 50 cytogenetically defined intervals along this chromosome (*73*) and genotyped on the CEPH reference families. The map extends from D16S85, which is within 170 to 430 kb of the 16p telomere (*10*), to D16S44, which is within 230 kb of the 16q telomere (*74*), and covers more than 99% of the physical length of this chromosome. The sex-average map is 162 cM long (133 cM in males, 199 cM in females). The framework genetic map includes 33 loci in an order that is compatible with an independently determined physical order on the cytogenetic map (*73*). The comprehensive genetic map of all 50 loci is anchored to the cytogenetic map. The average distance between markers is 3.3 cM. The present genetic map contains ten loci with minimum heterozygosity of 70% and six $(CA)_n$ repeat microsatellite markers, which are the first of many now being characterized for this chromosome (*75*). Comparison of the sex-specific recombination rates reveals that the female map is 1.5 times larger than the male map, which departs slightly from the 1.7 genome average (*38*). Recombination in distal 16p is greater in males than in females, and across the region containing the centromere, recombination is considerably suppressed in males compared with females (*76*). A detailed physical map of cosmid contigs is under construction by cosmid fingerprinting (*77*).

Chromosome 17

P. O'Connell[a], R. Plaetke[b], D. F. Barker[c], P. R. Fain[c], K. K. Kidd[d], M. Skolnick[c], J. Phillips[e], A. E. Bale[d], G. Vergnaud[f], C. Schwartz[g], J. L. Weber[h], O. W. McBride[i], L. L. Cavalli-Sforza[j], O. I. Balazs[k], J. Murray[l], M. F. Leppert[m], J.-M. Lalouel[m], R. L. White[m]

A previous map for chromosome 17 (*34*) has been extended with CEPH (V5) data to include 116 loci defined by 133 RFLP systems and five microsatellite markers assayed by PCR. The map spans 168 cM (137 cM in males and 200 cM in females) with 51 loci uniquely placed. The average marker spacing is 4 cM and the largest interval between markers on the sex-average map is 9.7 cM. Seventeen of the 51 unambiguously ordered markers qualify as "index markers" with heterozygosities of at least 70% (from a total of 21). Selection of 14 of these on the basis of optimal spacing provides a nearly complete index marker map of chromosome 17, and there are five microsatellite markers that can be assayed by PCR. New, highly polymorphic genetic markers have been placed in and around regions containing genes responsible for neurofibromatosis 1 (*NF1*) at 17q11.2; Charcot-Marie-Tooth (CMT) neuropathy; and familial breast cancer (*BRCA1*), which has been localized to 17q21 and linked to several loci shown on the map presented here (D17S250, *RARA*, D17S41) (*6*), and within several regions where loss of heterozygosity has been observed in various neoplasias.

The new map confirms the distribution of sex-specific differences in male and female recombination rates along chromosome 17 that was described previously (*78*). Although an excess of recombination in the telomeric regions is observed in males [for example, for the intervals D17S34–D17S499: $\chi^2 = 32.3$ (DOF = 1); D17S501–D17S775: $\chi^2 = 14.6$ (DOF = 1)], the recombination fractions are generally larger in females than in males between D17S506 and D17S501 [$\chi^2 = 129.2$ (DOF = 1)]. In the region between D17S499 and D17S506 the recombination frequencies do not differ significantly between males and females.

Chromosome 18

R. E. Straub[a], M. C. Speer[a], Y. Luo[a], K. Rojas[b], W. Shao[a], P. O'Connell[c], J. Overhauser[b], J. Ott[a], T. C. Gilliam[a]

The genetic map of chromosome 18 includes 14 microsatellite markers (12 dinucleotide and 2 tetranucleotide repeats) (*79*) and 2 RFLP markers that are uniquely placed with odds of 1000:1. Twelve of the microsatellites and one of the RFLPs have heterozygosities greater than 70%. The average heterozygosity of the markers included in the map is 72%. In addition, we have made provisional placements of five additional markers (three microsatellites and two RFLPs). The map lengths are 72 cM for males, 161 cM for females, and 109 cM for the sex-average distance. A preliminary framework map (*80*) was generated with CRI-MAP (*25*). The data were then examined by means of the CHROMPIC option of CRI-MAP for potential data errors, and individuals involved in double and higher order recombination events were regenotyped. The map was refined with the CILINK program (*81*) of the LINKAGE package [see (*82*) for details] and is supported over the next most likely order with odds >1000:1. The average distance between markers in the sex-average map is 7.3 cM, and the largest gap between markers on this map is 16.7 cM. Although this map is shorter than that reported by O'Connell *et al.* (*83*), the average distance between markers is less (7.3 versus 10.5 cM), and the average marker heterozygosity is greater (72 versus 49%). Analysis of the data for differences in the female:male map distance ratio (MDR) revealed an overall MDR of 2.5:1. In addition, there is evidence in favor of variability in female:male MDRs across the chromosome.

Chromosome 19

J. L. Weber[a], H. G. Harley[b], M. C. Speer[c]

The chromosome 19 baseline linkage map was built around a framework of 15 microsatellites and one RFLP (the marker at locus D19S20). Markers were chosen for the framework on the basis of high informativeness, position and spacing along the chromosome, and the ability to be typed by PCR. The framework was constructed primarily with the program package CRI-MAP (*25*), but pairwise LOD scores and CROSSMAP (*35*) were also utilized. The order for pairs of markers along the framework was supported by likelihood ratios (against inversion) of at least 10^{10}:1 and also by seven or more clear recombination events between each pair of markers. An additional set of 31 polymorphisms, some PCR-based but mainly RFLPs, including polymorphisms at 12 gene loci, was added to the framework in positions that were supported with odds of at least 1000:1 as determined by the maximum likelihood calculations. Duplicate typing of the dinucleotide repeat polymorphism at the *APOC2* locus and other error checking procedures resulted in an estimate of typing error for the PCR-based markers of approximately 0.5%. Female recombination rates exceeded male rates in the interior of the map from D19S177 to *HRC*, while the pter end of the map showed an excess of male recombination. The map is consistent with and extends previously published linkage maps for this chromosome (*84*).

Chromosome 20

T. P. Keith[a], K. Falls[a], D. W. Bowden[b], J. L. Weber[c], P. V. Gejman[d], J. Hazan[e], P. Phipps[a], K. Serino[a]

The sex-average map is 147 cM in length and consists of 50 loci, 33 of which were uniquely placed with global odds of 1000:1 and, with the exception of D20S40 and D20S18, local support of 1000:1. Forty-three of the markers are from the CEPH V5 database [26 of these were previously included in a map by Hazan *et al.* (*17*) and five additional markers are recently mapped microsatellite markers (one of these was originally typed by RFLPs]. D20S6, included in previous chromosome 20 maps (*12, 17, 85*) and previously designated a "reference marker" for chromosome 20 (*86*), was not included in the current map because of observed intralocus recombinants in three independent data sets. Twenty-six of the 50 markers on the map have heterozygosities of at least 70% and 34 are microsatellite markers that can be typed by PCR.

The map spans 162 cM in females and 135 cM in males. On the basis of a likelihood ratio test from two-point analyses, females show significantly ($P < 0.05$) higher recombination frequencies than males over much of the chromosome, including the regions spanned from D20S61–D20S58, D20S18–*SRC*, *PLC1–ADA*, and D20S33–D20S4. In one region (D20S25–*GNAS*) there was a significant excess of male recombination. The average marker spacing on the female and male maps is 5 and 4 cM, respectively, with the largest distance between two adjacent markers equal to 14 cM on the female map and 23 cM on the male map.

Chromosome 21

S. E. Antonarakis[a], A. Chakravarti[b], M. G. McInnis[a], V. Sharma[c], D. Avramopoulos[a], J. E. Blaschak[b], M. Litt[c], J.-L. Blouin[a]

The human chromosome 21 map represents a subset of 13 evenly spaced and highly informative polymorphic loci selected from a collection of more than 50 genetic markers. A comprehensive map of 42 polymorphic markers genotyped in CEPH pedigrees by PCR will be reported elsewhere (*87*). The map consists of 13 loci, of which 11 can be genotyped by PCR-based methods. The heterozygosity of these markers ranges from 60 to 95%, with 12 of the 13 markers having heterozygosities greater than 70%. The chromosome 21 map has a male genetic length of 57 cM, a female genetic length of 78 cM, and a sex-average genetic length of 67 cM. On the basis of the cytogenetic localization of the terminal loci (D21S120 and D21S112), we estimate that the genetic map spans almost the entire physical length of the long arm of the chromosome (39 Mb) (*38*). On the sex-average map the 12 marker intervals range from 3.2 to 7.9 cM, with an average spacing of 5.6 cM. Sex-specific differences in recombination frequency were examined along the chromosome arm by testing each interval. Significant sex differences were observed at the terminal intervals: D21S120–D21S11 where females showed greater recombination than males, and for the interval D21S171–D21S112 where males showed greater recombination than females. There appears to be excessive recombination toward the telomere of the chromosome. Linkage maps for chromosome 21 that contain polymorphic markers typed by Southern blotting in the CEPH or the Venezuelan reference pedigrees have been reported (*88*). The map presented here is considerably shorter than the previously published maps in CEPH pedigrees, presumably because rigorous error checking has eliminated false recombination events. The current map includes approximately 95% of the physical length of the chromosome and is comprised of highly informative, closely spaced markers.

Chromosome 22

J. L. Haines[a], K. H. Buetow[b], J. A. Trofatter[a]

The map consists of 22 loci (23 systems) and includes eight genes that span a sex-average distance of 98 cM. The male map (81 cM) is significantly shorter than the female map (115 cM) [$\chi^2 = 63.8$ (DOF = 21), $P < 0.005$], but only one interval (between *MB* and D22S102) demonstrates a sex-specific recombination difference that reaches statistical significance. Four markers with heterozygosities above 70% can be genotyped by PCR and will therefore be useful as "index markers." The remaining 19 markers are classical RFLPs. Comparison of our map to two others reported indicates that for all markers held in common [four with the map by Rouleau *et al.* (*89*) and 12

with the Dumanski *et al.* map (*33*)] the orders are identical and the distances are quite similar.

Chromosome X

J. C. Murray[a], S. J. Ludwigsen[b], K. H. Buetow[b]

The linkage map of the X chromosome contains 71 markers, a relatively modest number considering that this chromosome represents approximately 5% of the genome. Whereas the majority of markers are RFLP-based, there is now an increasing availability of microsatellite polymorphisms, which will greatly enhance the quality of this map over the next year. Fifteen markers in the map have heterozygosities of at least 70%, including 6 of the 20 microsatellites mapped (*90*). At the present time, the genetic length of 208 cM is similar to that of the chiasma-based (*38*) and previously published linkage maps (*12, 91*). Genetic markers developed from cloned telomeres have not yet been incorporated into the map. However, on the basis of the positions of cytogenetic tie points to the most distal markers from the linkage map (DXS207 and DXS52) and physical mapping data indicating that DXS52 lies within a few megabases of the q telomere (*92*), we estimate that approximately 95% of the physical length of the chromosome is contained within the genetic linkage map. Twenty-two markers are uniquely placed and there are five intervals with intermarker spacing greater than 15 cM, including a substantial genetic gap of 44 cM on the short arm. The extent of genotyping errors has not yet been ascertained since the CEPH database was used without further evaluation. A number of X chromosome mapping efforts have also been carried out by others, and substantial information, such as YAC physical mapping data and high-resolution genetic maps for several subregions of the X chromosome, is also available from the Genome Database (GDB) (*93*).

Discussion

The major difference between previously published maps and those presented here (and also *17, 39, 54, 69*) is the informativeness and type of marker now being used. For example, a genome map published 5 years ago (*12*) consisted almost entirely of RFLPs (397, plus five protein polymorphisms), and only 7% of these markers (*28*) had heterozygosities of 70% or greater. In the current map 339 markers are microsatellites and they constitute more than 50% of markers with heterozygosity of at least 70%. Although 80% of the markers in the map reported here are RFLPs, the rapid integration of microsatellites [the first of which were reported just 3 years ago (*18*)] predicts that they will become the dominant markers on the map. The popularity of microsatellites over RFLPs is due to their high degree of informativeness, convenience of assay by PCR, relatively even distribution throughout the genome, and availability (from publication of primer sequences).

The most densely mapped chromosomes are 7 and 17, with 112 and 116 loci mapped, respectively. Considering that chromosome 17 is about 50% as large in predicted physical distance, but comparable in estimated genetic length (based on chiasma, chromosome 17 is 196 cM and chromosome 7 is 178 cM), it constitutes the most densely mapped chromosome per megabase spanned. Except for chromosomes 3 and 5 (where the average marker spacing is 6.4 and 7 cM, respectively), each chromosome map has an average marker spacing of less than 5 cM.

As the Y chromosome has no homolog and only undergoes genetic exchange at the pseudoautosomal region on Yp with an Xpter segment, a genetic map for this part of the genome is not presented. Even so, the pseudoautosomal region has provided an opportunity to compare genetic to physical distance and to study sex-specific recombination. The genetic distance of the pseudoautosomal region is estimated at 4 to 18 cM in female meioses and at 50 cM in male meioses (no more than several megabases) (*94*).

All of the chromosome maps consist of continuous linkage groups. In a few cases (chromosomes 2q, 4p, 7q, 8p, 14q, 16p, and 16q) genetic map closure has been achieved through telomeric polymorphisms, but in the absence of clone-based physical maps, most of our estimates of physical genome coverage rely on cytogenetic assignments of markers to Giemsa-stained metaphase chromosomes or on fractional length measurements obtained in similar FISH experiments. Traditional cytogenetic banding patterns have relatively low resolution (for example, approximately 6 to 10 Mb per band) and are often useless as a check for the order of closely linked genetic markers. In addition, it is not known whether dark staining and light staining bands have equal DNA content. However newer methods of interphase mapping have allowed the orientation of closely linked markers on the physical map and could be important in resolving confusing orders in genetic data. For the X chromosome (although the telomeres are not represented in the map presented here), the long-range physical maps of the p and q telomere regions (*92, 95*) have made possible estimates of physical coverage for this map. When only cytogenetic mapping information is available, more conservative estimates of coverage have been made. Undoubtedly extensive physical maps will be forthcoming in the near future (*96*), but we must consider that in genome screens without physical and genetic telomere markers, it is difficult to estimate the remaining genetic distance. Evidence that gene sequences extend to the termini of chromosomes is provided from physical mapping of the globin locus on 16pter and the Huntington's disease locus in terminal 4p, which underscores the importance of ongoing studies to achieve closure of the maps. The only additional regions that await more detailed mapping are the centromeres and the short arms of the acrocentric chromosomes (chromosomes 13, 14, 15, 21, and 22). However, except for ribosomal RNA genes, it is unlikely that many additional genes reside in these regions since they appear to consist almost entirely of α- and β-alphoid repeat elements (*62, 97*).

One limitation of the current chromosome maps is the low number and uneven representation of genes and expressed sequences. For example, more than 1500 cloned genes have been reported (*86*) yet less than 20% have been incorporated into the genetic maps reported here. This is mainly due to the low rate of RFLP polymorphism previously found at these loci, and it is expected that since microsatellites have been found in abundance within introns or nearby gene loci, this deficiency will be corrected. In fact, of the 279 gene loci incorporated in the map, 66 are now represented by microsatellites (ten of these also have associated RFLPs). One important reason for precisely localizing genes in the maps is to recognize and test them as candidate disease genes. It is worth noting that although glucokinase has long been considered a candidate gene for diabetes susceptibility, it was not until recently, when highly informative microsatellite markers at this locus became available, that the appropriate studies linking the disease phenotype with the gene were made possible (*7, 98*).

The genome map presented here covers an autosomal sex-average distance of 4702 cM, which is about 20% larger than the mean length estimated from chiasma counts (3734 cM). Since we estimate that as much as 10% of the physical length of the genome is not included in the map, we expect that the apparent map inflation is likely due to genotyping errors. Several groups have estimated error rates from comparisons of markers that were typed in duplicate (for example, see chromosome 1 description). On the basis of these observations of a 0.5 to 1.0% error rate per polymorphic system

typed (a 0.5- to 1.0-cM increase per system, and a total of 1604 autosomal systems), the overall increase in autosomal map size would be about 800 to 1600 cM, which is within the range of the map length increase that is observed.

We must address the likelihood that genotyping errors leading to map expansion may also indicate potentially incorrect marker orders. Buetow's Monte Carlo simulation analysis of linkage data indicated that as multipoint maps approach a 1-cM interlocus resolution, even a relatively low 0.5% typing error rate would result in 5% incorrect marker orders (for maps constructed with LOD 3 criteria) (99). However, genotyping error rates of even 1.5% had minimal effect in producing incorrect map orders for maps with less (2 cM) resolution (99). In general, the data sets used to produce the current maps were not rigorously checked, and in the future marker orders for regions with high marker densities should be rechecked by duplicate typings, particularly where clustering of apparent recombinant events in families is observed (*100*).

The chromosome maps presented here, particularly those with microsatellite markers, will be useful for designing linkage studies in search of genes responsible for heritable disorders. A subset of markers that are highly informative and relatively evenly spaced (for example, at approximately 15-cM intervals) can be conveniently selected by examination of the map graphics and Table 1 (see pages 148 to 159; it also references the experimental conditions for the markers). The chromosome 21 map shown here is designed for this type of project. Eleven of the 13 markers in the map (chosen from a much larger collection) can be assayed by PCR, and the intermarker spacing is less than 10 cM. Maps that are dominated by RFLPs will also be useful to quickly place new markers. Because these maps depict a comprehensive collection of markers available for given regions, they are useful for more detailed mapping once a disease gene has been subregionally localized. Since most microsatellite markers are highly informative, simply genotyping a new marker in five to eight CEPH families (*101*) should be sufficient to quickly place it in the context of the current maps (that is, from a two-point analysis). At the present time the maps provide a "baseline" upon which future mapping efforts will be focused. It is expected that "index maps" for each of the chromosomes will be completed within the next year and these will provide even better tools for disease gene searches. Genetic maps are never complete. Inherent in the activity is a continuous process of modification as new markers are developed and as existing data are reexamined and corrected. We are now reaching a point in the genome project where, for the first time, as in other model organisms (for example, *102*), human genetic and clone-based mapping over relatively large distances will converge, and it is anticipated full integration of genetic, cytogenetic, and physical mapping information will be possible, thereby providing a new "view" of the genome upon which to base future biological studies.

Fig. 1 (pages 77 to 83). Genetic linkage maps for 23 human chromosomes. Graphical representations are shown for each of the 22 autosomes and the X chromosome (*103*). The cumulative length for each sex-average genetic map is indicated at the top of each map graphic (in centimorgans; recombination fractions were converted to centimorgans by means of Kosambi mapping function). In order to best illustrate the map intervals and display the marker names, the chromosomes are not strictly represented according to their physical and genetic size. Loci uniquely placed with odds for order of at least 1000:1 are tethered to the map (to the right of the vertical map line) and are represented by HGM gene names and D segment numbers where available. A "*" indicates loci with heterozygosities of at least 70%. Microsatellite markers assayed by PCR are shown in italics. The intermarker spacing in centimorgans is indicated to the left of the map line. The sex-average map also shows markers that are not uniquely ordered. The genetic intervals for these markers are indicated by solid vertical lines to the left of the corresponding intervals on the map line. These intervals represent the placement of the markers at 1000:1 odds except for chromosome 3 (only the most likely intervals for placement at 100:1 odds are shown). The marker names are located to the left of the interval lines, and when more than one marker maps to the same interval, the markers are listed (the order for these groups of markers with respect to each other has not been determined). Dashed interval lines indicate excluded regions for the marker. Representative tie points between markers included in the genetic maps that have also been cytogenetically mapped are drawn between the sex-average map and the chromosomal idiogram (to the right of the sex-average map). Brackets indicate the physical map position of markers based on cytogenetic mapping data (referenced in Table 1; see pages 148 to 159). Arrows at the end points of tie lines between the idiogram and the genetic maps indicate a mapped polymorphism from a cloned telomere segment. The idiograms depict the Giemsa staining pattern at 550-band resolution for metaphase chromosomes [ISCN 550 G-bands (*37*)], except for chromosome 16, which illustrates 850-band resolution. Loci that may be in an inverted order are indicated with a brace (}) on the sex-average map. For the chromosome 5 map graphic, a "°" indicates the primary map markers used in the early stages of map construction. Chromosomes 6 and 7 have brackets on the genetic map lines indicating regions spanned by the *HLA* and *TCRB* gene clusters, both of which have intralocus recombination (detailed genetic maps for these regions are not shown).

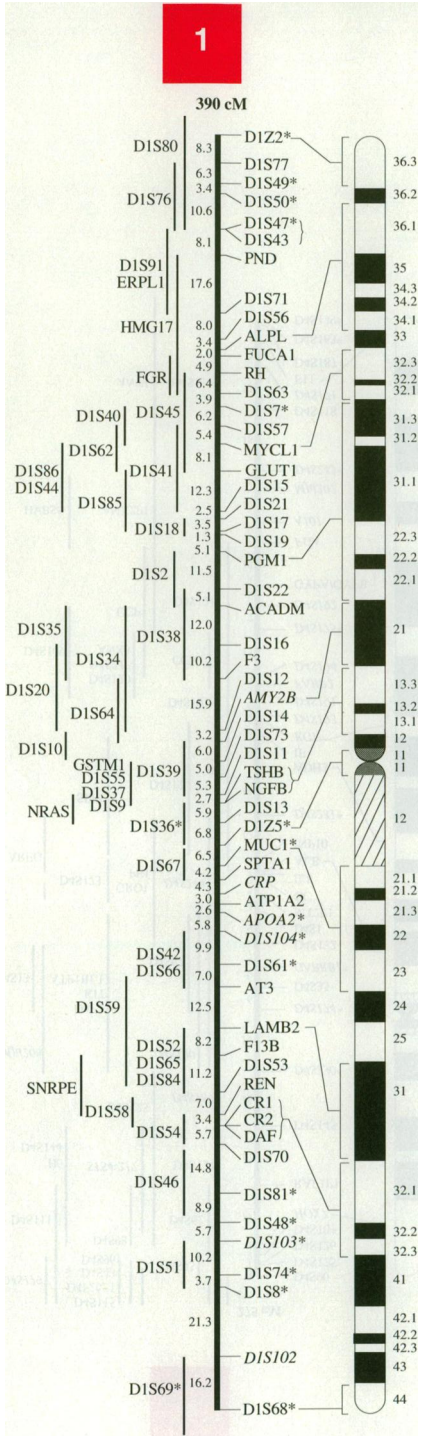
1
390 cM
D1S80
D1S76
D1S91
ERPL1
HMG17
FGR
D1S40
D1S45
D1S62
D1S86
D1S44
D1S41
D1S85
D1S18
D1S2
D1S35
D1S38
D1S34
D1S20
D1S64
D1S10
GSTM1
D1S55
D1S37
D1S9
NRAS
D1S39
D1S36*
D1S67
D1S42
D1S66
D1S59
D1S52
D1S65
D1S84
SNRPE
D1S58
D1S54
D1S46
D1S51
D1S69*
D1Z2*
D1S77
D1S49*
D1S50*
D1S47*
D1S43
PND
D1S71
D1S56
ALPL
FUCA1
RH
D1S63
D1S7*
D1S57
MYCL1
GLUT1
D1S15
D1S21
D1S17
D1S19
PGM1
D1S22
ACADM
D1S16
F3
D1S12
AMY2B
D1S14
D1S73
D1S11
TSHB
NGFB
D1S13
D1Z5*
MUC1*
SPTA1
CRP
ATP1A2
APOA2*
D1S104*
D1S61*
AT3
LAMB2
F13B
D1S53
REN
CR1
CR2
DAF
D1S70
D1S81*
D1S48*
D1S103*
D1S74*
D1S8*
D1S102
D1S68*

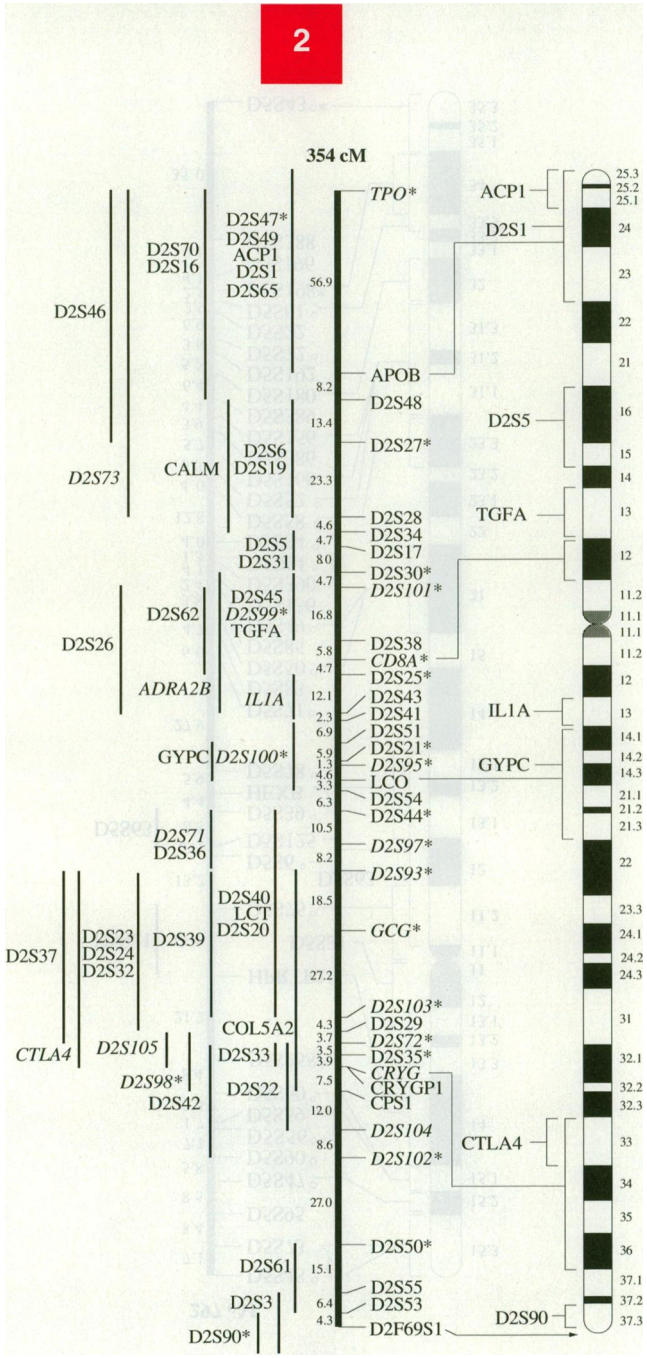
2
354 cM
D2S46
D2S70
D2S16
D2S73
CALM
D2S6
D2S19
D2S5
D2S31
D2S62
D2S26
ADRA2B
D2S45
D2S99*
TGFA
IL1A
GYPC
D2S100*
D2S71
D2S36
D2S37
D2S23
D2S24
D2S32
D2S39
CTLA4
D2S105
D2S98*
D2S42
D2S40
LCT
D2S20
COL5A2
D2S33
D2S22
D2S61
D2S3
D2S90*
D2S47*
D2S49
ACP1
D2S1
D2S65
TPO*
APOB
D2S48
D2S27*
D2S28
D2S34
D2S17
D2S30*
D2S101*
D2S38
CD8A*
D2S25*
D2S43
D2S41
D2S51
D2S21*
D2S95*
LCO
D2S54
D2S44*
D2S97*
D2S93*
GCG*
D2S103*
D2S29
D2S72*
D2S35*
CRYG
CRYGP1
CPS1
D2S104
D2S102*
D2S50*
D2S55
D2S53
D2F69S1
ACP1
D2S1
D2S5
TGFA
IL1A
GYPC
CTLA4
D2S90

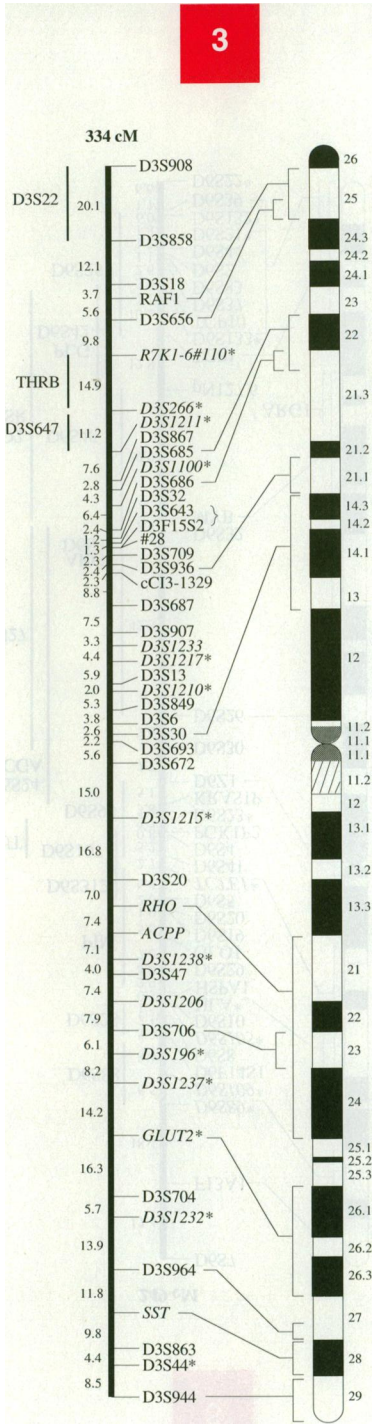
3
334 cM
D3S22
THRB
D3S647
D3S908
D3S858
D3S18
RAF1
D3S656
R7K1-6#110*
D3S266*
D3S1211*
D3S867
D3S685
D3S1100*
D3S686
D3S32
D3S643
D3F15S2
#28
D3S709
D3S936
cCI3-1329
D3S687
D3S907
D3S1233
D3S1217*
D3S13
D3S1210*
D3S849
D3S6
D3S30
D3S693
D3S672
D3S1215*
D3S20
RHO
ACPP
D3S1238*
D3S47
D3S1206
D3S706
D3S196*
D3S1237*
GLUT2*
D3S704
D3S1232*
D3S964
SST
D3S863
D3S44*
D3S944

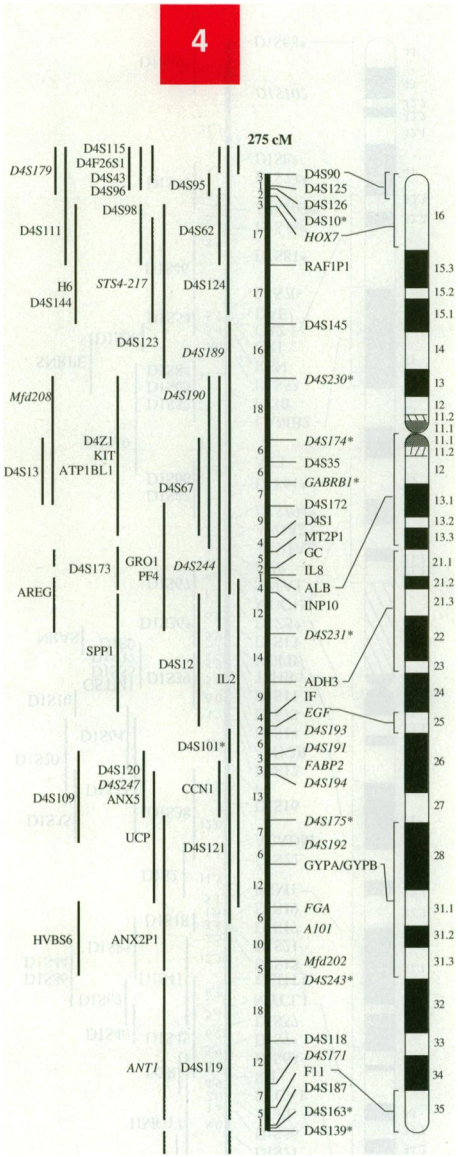
4
275 cM
D4S115
D4F26S1
D4S43
D4S96
D4S95
D4S98
D4S62
D4S111
H6
D4S144
STS4-217
D4S124
D4S123
D4S189
D4S190
Mfd208
D4Z1
KIT
ATP1BL1
D4S13
D4S67
D4S173
GRO1
PF4
D4S244
AREG
SPP1
D4S12
IL2
D4S101*
D4S120
D4S247
ANX5
D4S109
CCN1
UCP
D4S121
HVBS6
ANX2P1
ANT1
D4S119
D4S90
D4S125
D4S126
D4S10*
HOX7
RAF1P1
D4S145
D4S230*
D4S174*
D4S35
GABRB1*
D4S172
D4S1
MT2P1
GC
IL8
ALB
INP10
D4S231*
ADH3
IF
EGF
D4S193
D4S191
FABP2
D4S194
D4S175*
D4S192
GYPA/GYPB
FGA
A101
Mfd202
D4S243*
D4S118
D4S171
F11
D4S187
D4S163*
D4S139*

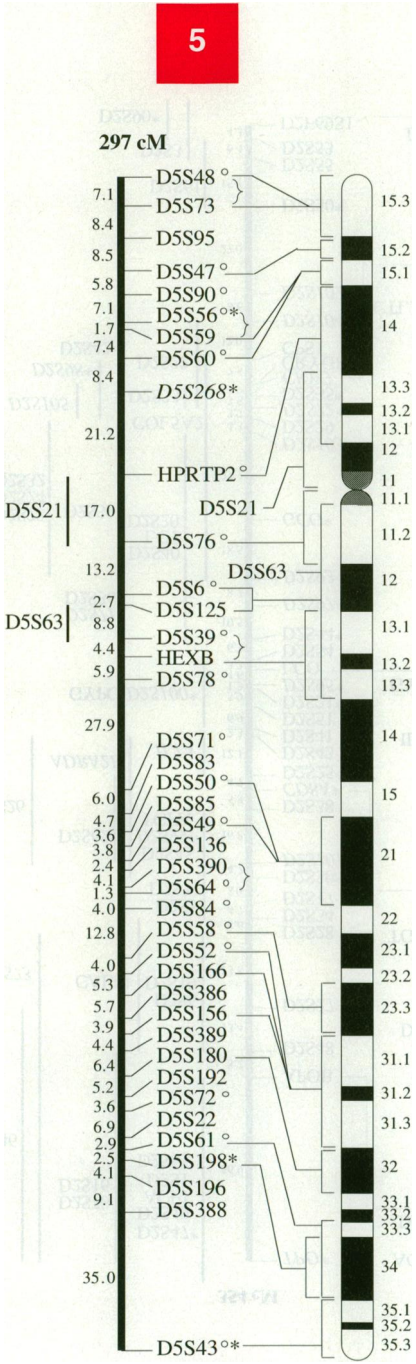
5
297 cM
D5S48 °
D5S73
D5S95
D5S47 °
D5S90 °
D5S56 °*
D5S59
D5S60 °
D5S268*
HPRTP2 °
D5S21
D5S21
D5S76 °
D5S63
D5S6 °
D5S125
D5S63
D5S39 °
HEXB
D5S78 °
D5S71 °
D5S83
D5S50 °
D5S85
D5S49 °
D5S136
D5S390
D5S64 °
D5S84 °
D5S58 °
D5S52 °
D5S166
D5S386
D5S156
D5S389
D5S180
D5S192
D5S72 °
D5S22
D5S61 °
D5S198*
D5S196
D5S388
D5S43 °*

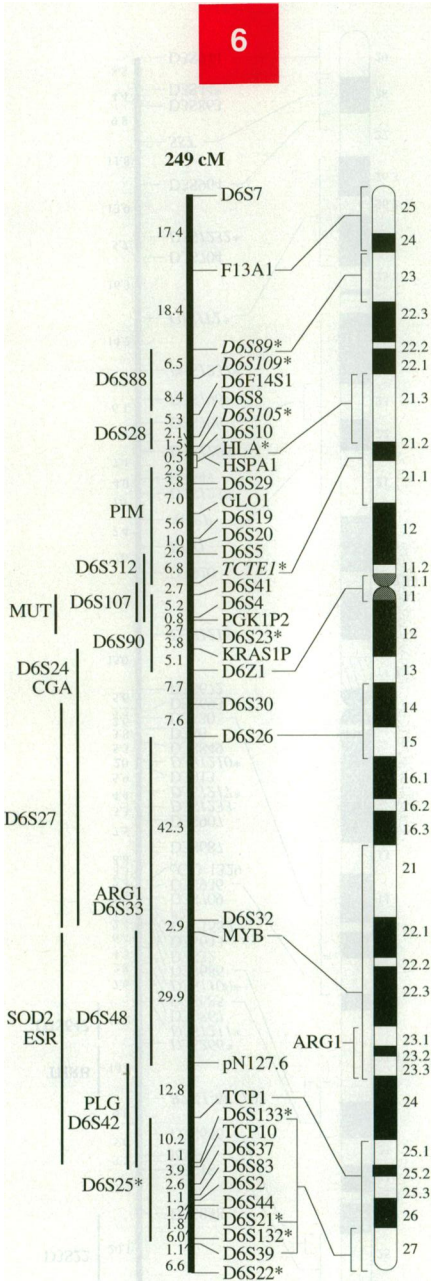
6
249 cM
D6S7
F13A1
D6S89*
D6S109*
D6S88
D6F14S1
D6S8
D6S105*
D6S28
D6S10
HLA*
HSPA1
PIM
D6S29
GLO1
D6S19
D6S20
D6S5
TCTE1*
D6S312
D6S41
MUT
D6S107
D6S4
PGK1P2
D6S90
D6S23*
KRAS1P
D6S24
CGA
D6Z1
D6S30
D6S26
D6S27
ARG1
D6S33
D6S32
MYB
SOD2
ESR
D6S48
ARG1
pN127.6
PLG
D6S42
TCP1
D6S133*
TCP10
D6S37
D6S83
D6S25*
D6S2
D6S44
D6S21*
D6S132*
D6S39
D6S22*

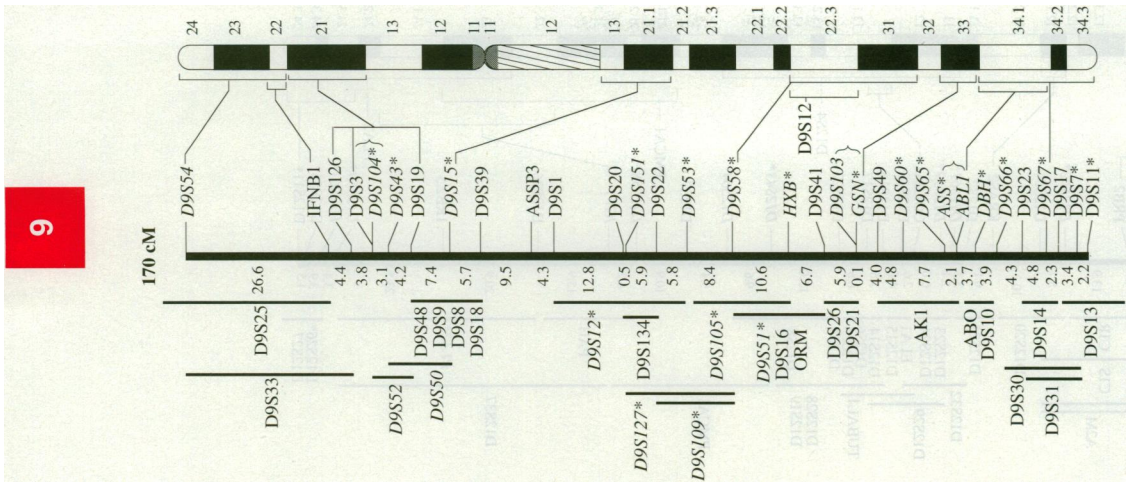
9
170 cM
D9S54
IFNB1
D9S126
D9S3
D9S104*
D9S43*
D9S19
D9S15*
D9S39
ASSP3
D9S1
D9S20
D9S151*
D9S22
D9S53*
D9S58*
HXB*
D9S12
D9S41
D9S103
GSN*
D9S49
D9S60*
D9S65*
ASS*
ABL1
DBH*
D9S66*
D9S23
D9S67*
D9S17
D9S7*
D9S11*
D9S25
D9S33
D9S52
D9S50
D9S48
D9S9
D9S8
D9S18
D9S12*
D9S134
D9S127*
D9S109*
D9S105*
D9S551*
D9S16
ORM
D9S26
D9S21
AK1
ABO
D9S10
D9S30
D9S31
D9S14
D9S13

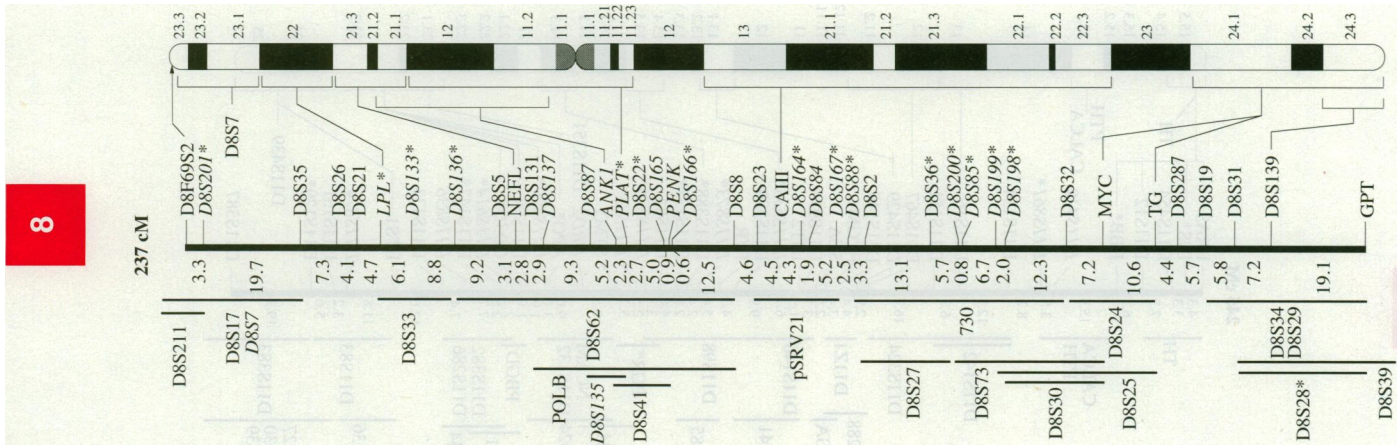
8
237 cM
D8F69S2
D8S201*
D8S7
D8S35
D8S26
D8S21
LPL*
D8S133*
D8S136*
D8S5
NEFL
D8S131
D8S137
D8S587
ANK1
PLAT*
D8S22*
D8S165
PENK
D8S166*
D8S8
D8S23
CAIII
D8S164*
D8S84
D8S167*
D8S88*
D8S2
D8S36*
D8S200*
D8S85*
D8S199*
D8S198*
D8S32
MYC
TG
D8S287
D8S19
D8S31
D8S139
GPT
D8S211
D8S17
D8S7
D8S33
POLB
D8S62
D8S135*
D8S41
pSRV21
D8S27
730
D8S573
D8S30
D8S24
D8S25
D8S34
D8S29
D8S28*
D8S39

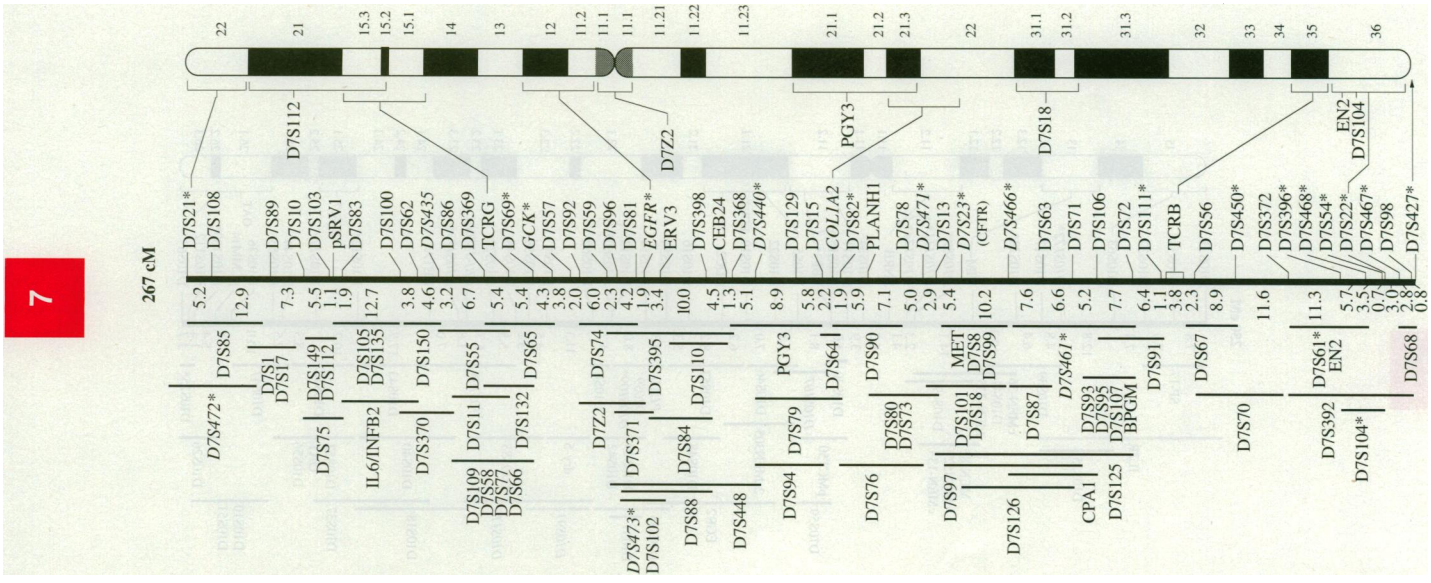
7
267 cM
D7S21*
D7S108
D7S112
D7S89
D7S10
D7S103
pSRV1
D7S83
D7S100
D7S62
D7S435
D7S86
D7S369
TCRG
D7S69*
GCK*
D7S57
D7S92
D7S59
D7S96
D7S81
EGFR*
ERV3
D7S398
CEB24
D7S368
D7S440*
D7S129
D7S15
COLIA2
D7S82*
PLANH1
D7S78
D7S471*
D7S13
D7S523*
(CFTR)
D7S466*
D7S563
D7S71
D7S106
D7S72
D7S111*
TCRB
D7S556
D7S450*
D7S372
D7S396*
D7S468*
D7S554*
D7S22*
D7S467*
D7S598
D7S427*
EN2
D7S104
PGY3
D7S18
D7S472*
D7S85
D7S1
D7S17
D7S149
D7S112
D7S75
D7S105
D7S135
IL6/INFB2
D7S150
D7S370
D7S109
D7S558
D7S577
D7S566
D7S11
D7S555
D7S132
D7S65
D7S722
D7S74
D7S371
D7S473*
D7S102
D7S395
D7S84
D7S88
D7S110
D7S448
D7S94
D7S79
PGY3
D7S64
D7S76
D7S80
D7S73
D7S90
D7S97
D7S101
D7S18
MET
D7S8
D7S99
D7S126
D7S87
D7S461*
CPA1
D7S93
D7S95
D7S107
BPGM
D7S125
D7S91
D7S67
D7S570
D7S392
D7S104*
D7S61*
EN2
D7S68

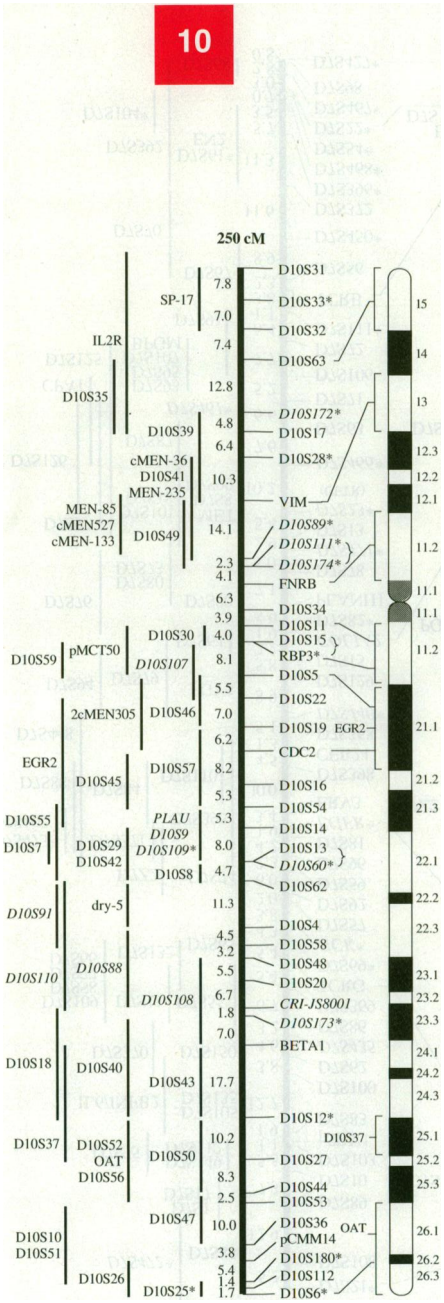
10
250 cM
D10S31
D10S33*
D10S32
D10S63
D10S172*
D10S17
D10S28*
VIM
D10S89*
D10S111*
D10S174*
FNRB
D10S34
D10S11
D10S15
RBP3*
D10S5
D10S22
D10S19
CDC2
D10S16
D10S54
D10S14
D10S13
D10S60*
D10S62
D10S4
D10S58
D10S48
D10S20
CRI-JS8001
D10S173*
BETA1
D10S12*
D10S37
D10S27
D10S44
D10S53
D10S36
pCMM14
D10S180*
D10S112
D10S6*
OAT
EGR2
SP-17
IL2R
D10S35
D10S39
cMEN-36
D10S41
MEN-235
MEN-85
cMEN527
cMEN-133
D10S49
D10S30
D10S59
pMCT50
D10S107
2cMEN305
D10S46
EGR2
D10S45
D10S57
D10S55
PLAU
D10S9
D10S7
D10S29
D10S109*
D10S42
D10S8
D10S91
dry-5
D10S110
D10S88
D10S108
D10S18
D10S40
D10S43
D10S37
D10S52
OAT
D10S56
D10S50
D10S47
D10S10
D10S51
D10S26
D10S25*
15
14
13
12.3
12.2
12.1
11.2
11.1
11.1
11.2
21.1
21.2
21.3
22.1
22.2
22.3
23.1
23.2
23.3
24.1
24.2
24.3
25.1
25.2
25.3
26.1
26.2
26.3

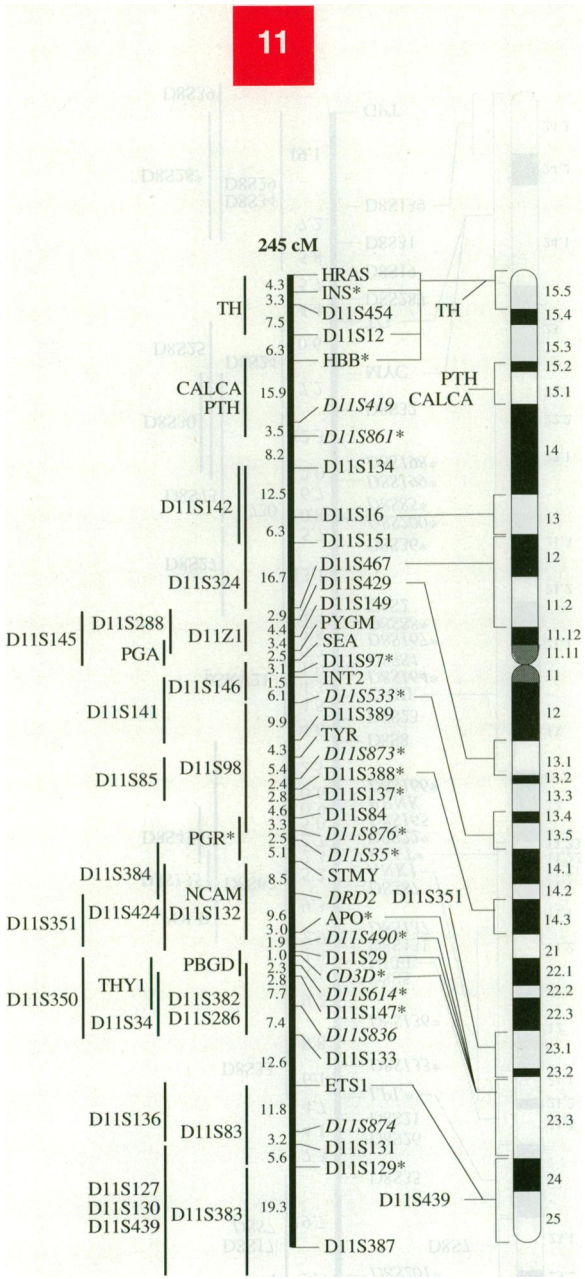
11
245 cM
HRAS
INS*
D11S454
D11S12
HBB*
D11S419
D11S861*
D11S134
D11S16
D11S151
D11S467
D11S429
D11S149
PYGM
SEA
D11S97*
INT2
D11S533*
D11S389
TYR
D11S873*
D11S388*
D11S137*
D11S84
D11S876*
D11S35*
STMY
DRD2
APO*
D11S490*
D11S29
CD3D*
D11S614*
D11S147*
D11S836
D11S133
ETS1
D11S874
D11S131
D11S129*
D11S439
D11S387
TH
PTH
CALCA
D11S142
D11S324
D11S145
D11S288
PGA
D11Z1
D11S146
D11S141
D11S85
D11S98
PGR*
D11S384
NCAM
D11S351
D11S424
D11S132
PBGD
D11S350
THY1
D11S382
D11S34
D11S286
D11S136
D11S83
D11S127
D11S130
D11S439
D11S383
D11S351
15.5
15.4
15.3
15.2
15.1
14
13
12
11.2
11.12
11.11
11
12
13.1
13.2
13.3
13.4
13.5
14.1
14.2
14.3
21
22.1
22.2
22.3
23.1
23.2
23.3
24
25

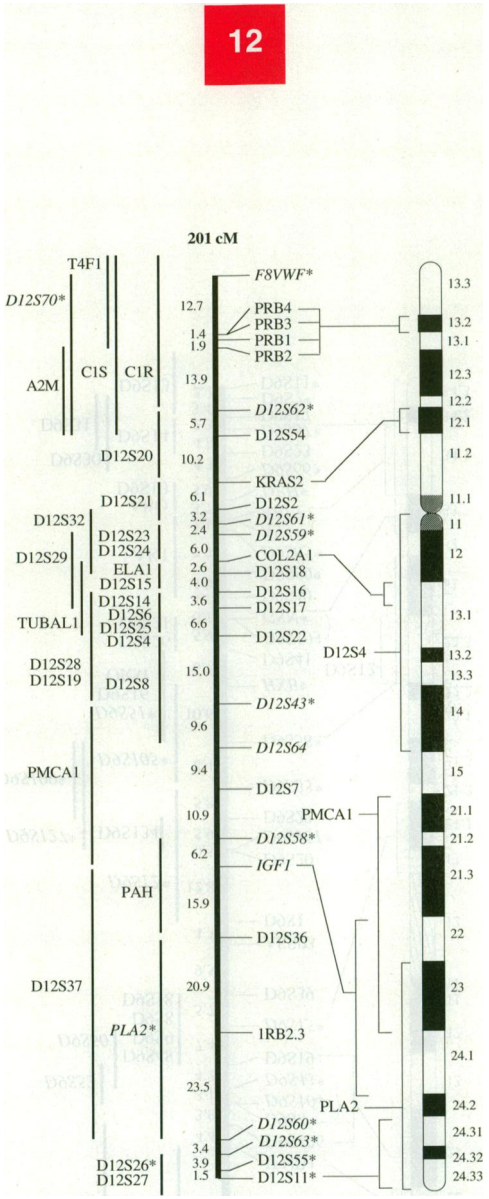
12
201 cM
T4F1
D12S70*
A2M
C1S
C1R
D12S20
D12S21
D12S32
D12S23
D12S24
D12S29
ELA1
D12S15
D12S14
D12S6
TUBAL1
D12S25
D12S4
D12S28
D12S19
D12S8
PMCA1
PAH
D12S37
PLA2*
D12S26*
D12S27
F8VWF*
PRB4
PRB3
PRB1
PRB2
D12S62*
D12S54
KRAS2
D12S2
D12S61*
D12S59*
COL2A1
D12S18
D12S16
D12S17
D12S22
D12S43*
D12S64
D12S7
D12S58*
IGF1
D12S36
1RB2.3
PLA2
D12S60*
D12S63*
D12S55*
D12S11*
13.3
13.2
13.1
12.3
12.2
12.1
11.2
11.1
11
12
13.1
13.2
13.3
14
15
21.1
21.2
21.3
22
23
24.1
24.2
24.31
24.32
24.33

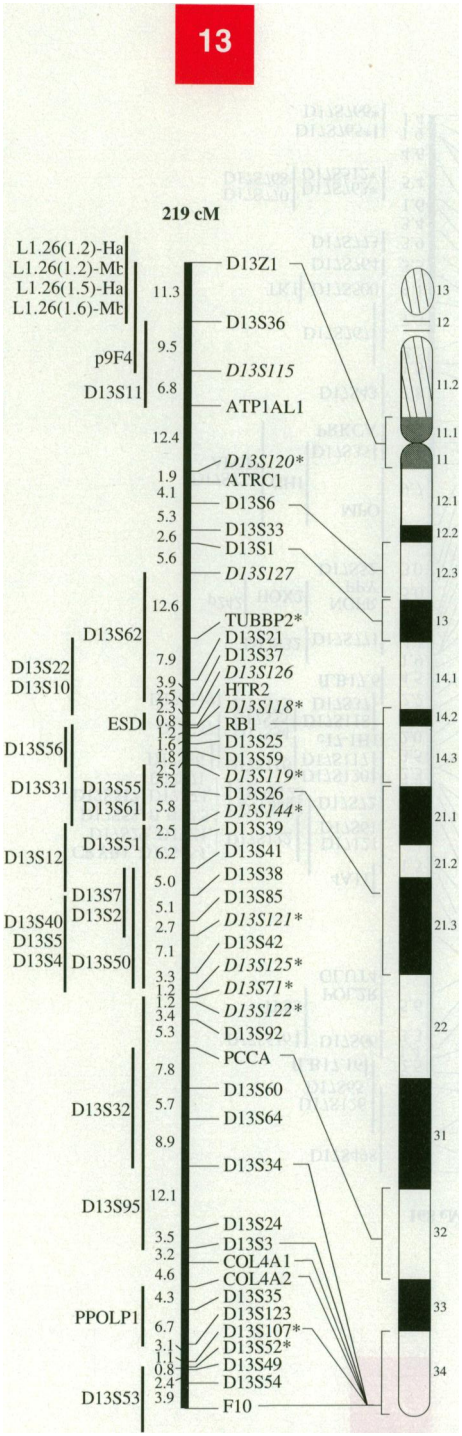
13
219 cM
L1.26(1.2)-Ha
L1.26(1.2)-Mb
L1.26(1.5)-Ha
L1.26(1.6)-Mb
D13Z1
D13S36
p9F4
D13S11
D13S115
ATP1AL1
D13S120*
ATRC1
D13S6
D13S33
D13S1
D13S127
D13S62
TUBBP2*
D13S21
D13S37
D13S22
D13S10
D13S126
HTR2
D13S118*
ESD
RB1
D13S56
D13S25
D13S59
D13S119*
D13S31
D13S55
D13S61
D13S26
D13S144*
D13S12
D13S51
D13S39
D13S41
D13S7
D13S2
D13S38
D13S85
D13S40
D13S5
D13S4
D13S50
D13S121*
D13S42
D13S125*
D13S71*
D13S122*
D13S92
PCCA
D13S32
D13S60
D13S64
D13S34
D13S95
D13S24
D13S3
COL4A1
COL4A2
PPOLP1
D13S35
D13S123
D13S107*
D13S52*
D13S49
D13S54
D13S53
F10

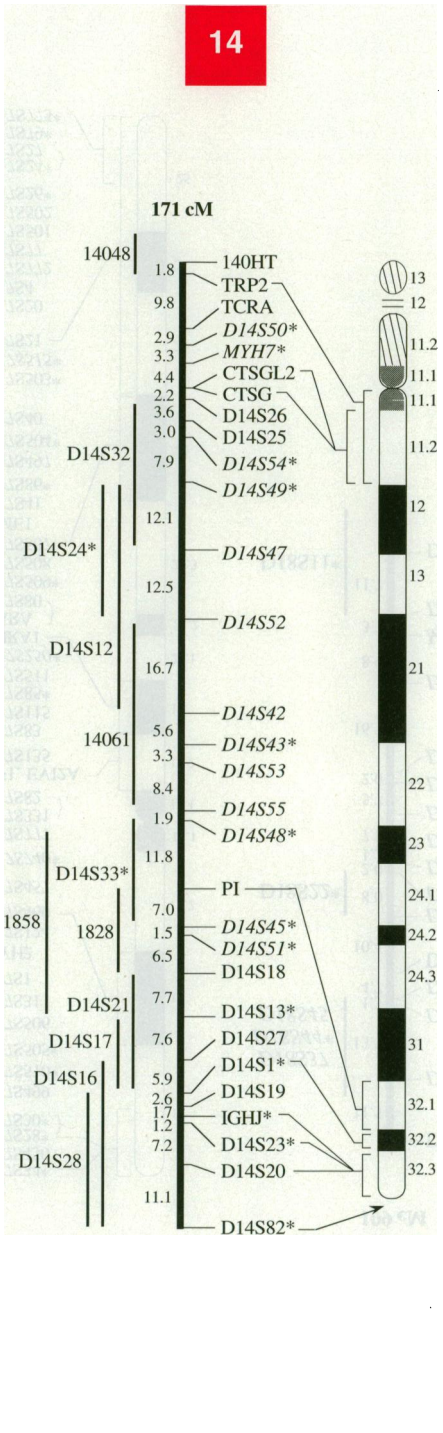
14
171 cM
14048
140HT
TRP2
TCRA
D14S50*
MYH7*
CTSGL2
CTSG
D14S26
D14S25
D14S32
D14S54*
D14S49*
D14S24*
D14S47
D14S52
D14S12
D14S42
14061
D14S43*
D14S53
D14S55
D14S48*
D14S33*
1858
1828
PI
D14S45*
D14S51*
D14S18
D14S21
D14S13*
D14S17
D14S27
D14S16
D14S1*
D14S19
IGHJ*
D14S23*
D14S28
D14S20
D14S82*

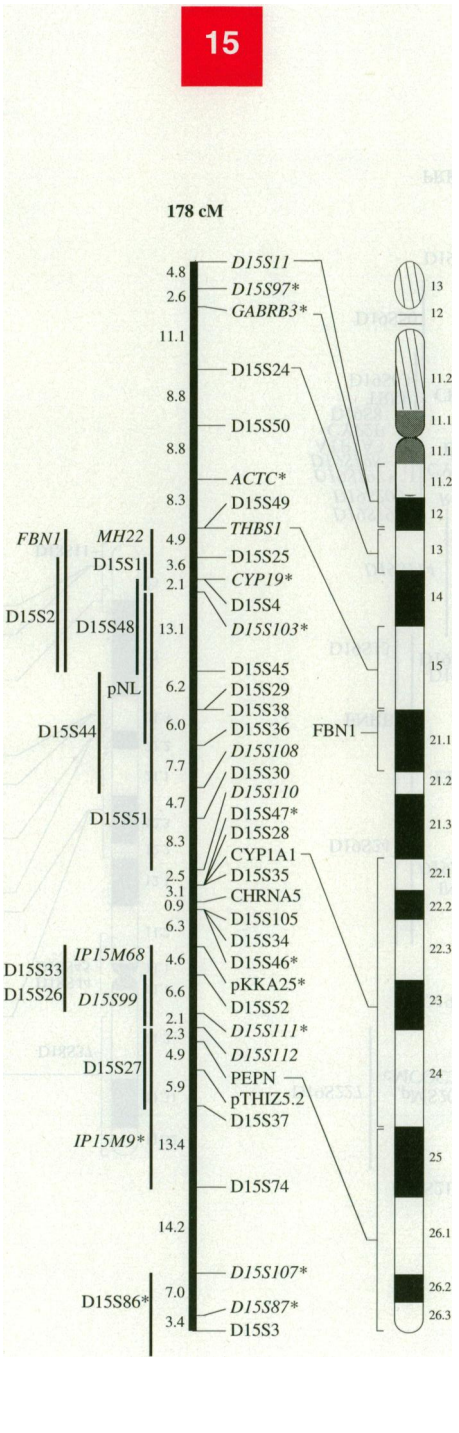
15
178 cM
D15S11
D15S97*
GABRB3*
D15S24
D15S50
ACTC*
D15S49
THBS1
FBN1
MH22
D15S1
D15S25
CYP19*
D15S2
D15S4
D15S48
D15S103*
pNL
D15S45
D15S29
D15S44
D15S38
D15S36
FBN1
D15S108
D15S30
D15S110
D15S51
D15S47*
D15S28
CYP1A1
D15S35
CHRNA5
D15S105
D15S34
D15S33
IP15M68
D15S46*
D15S26
D15S99
pKKA25*
D15S52
D15S111*
D15S27
D15S112
PEPN
pTHIZ5.2
IP15M9*
D15S37
D15S74
D15S107*
D15S86*
D15S87*
D15S3

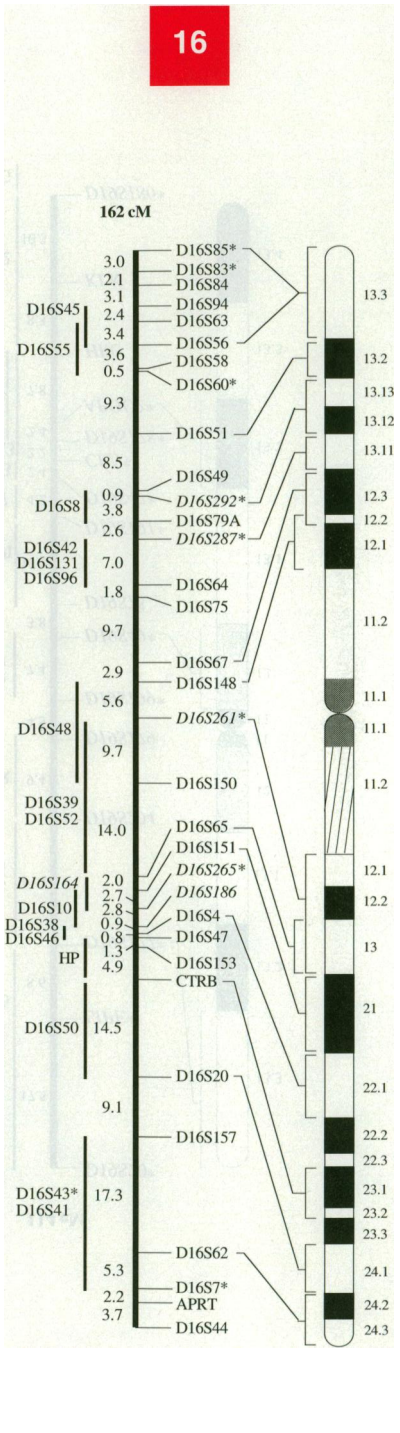
16
162 cM
D16S85*
D16S83*
D16S84
D16S45
D16S94
D16S63
D16S55
D16S56
D16S58
D16S60*
D16S51
D16S49
D16S8
D16S292*
D16S79A
D16S287*
D16S42
D16S131
D16S96
D16S64
D16S75
D16S67
D16S148
D16S261*
D16S48
D16S150
D16S39
D16S52
D16S65
D16S151
D16S265*
D16S164
D16S186
D16S10
D16S38
D16S4
D16S46
D16S47
HP
D16S153
CTRB
D16S50
D16S20
D16S157
D16S43*
D16S41
D16S62
D16S7*
APRT
D16S44

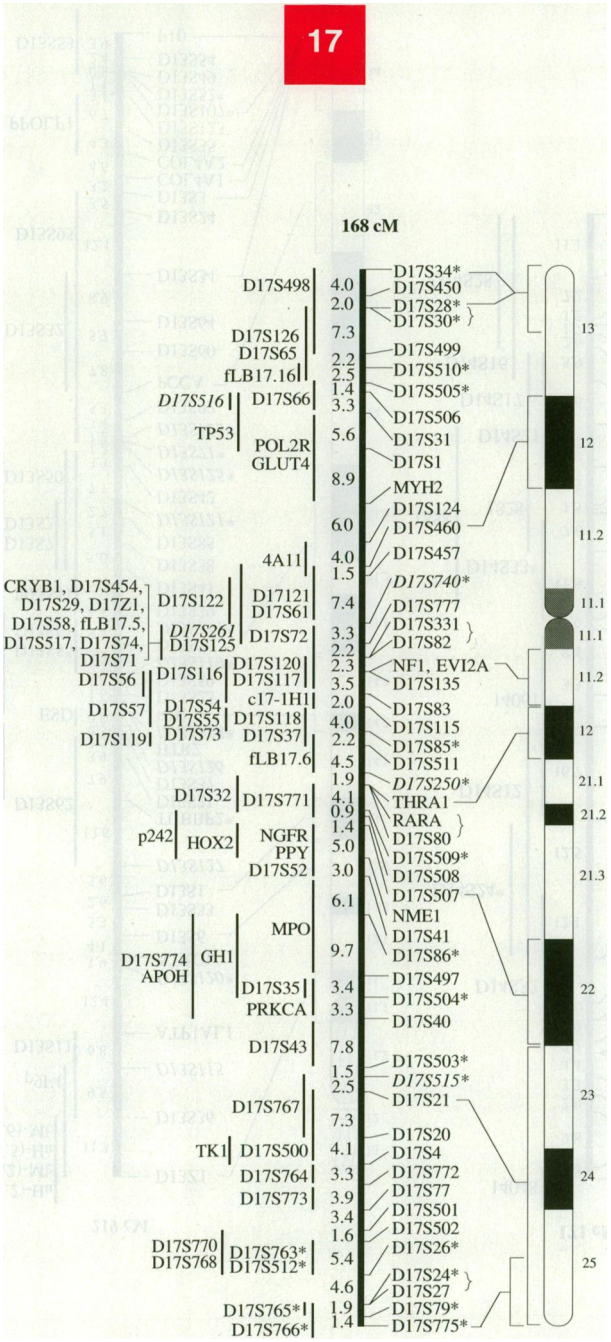
17
168 cM
D17S498
4.0
2.0
D17S34*
D17S450
D17S28*
D17S30*
13
D17S126
D17S65
7.3
D17S499
fLB17.16
2.2
2.5
D17S510*
1.4
D17S505*
D17S516
D17S66
3.3
D17S506
TP53
5.6
D17S31
POL2R
GLUT4
D17S1
12
8.9
MYH2
6.0
D17S124
D17S460
11.2
4A11
4.0
D17S457
1.5
D17S740*
CRYB1, D17S454,
D17S29, D17Z1,
D17S58, fLB17.5,
D17S517, D17S74,
D17S122
D17121
D17S61
7.4
D17S777
D17S331
11.1
D17S261
D17S125
D17S72
3.3
2.2
D17S82
11.1
D17S71
D17S56
D17S116
D17S120
D17S117
2.3
3.5
NF1, EVI2A
D17S135
11.2
D17S57
D17S54
c17-1H1
2.0
D17S83
D17S55
D17S118
4.0
D17S115
D17S119
D17S73
D17S37
2.2
D17S85*
fLB17.6
4.5
D17S511
12
1.9
D17S250*
21.1
D17S32
D17S771
4.1
THRA1
0.9
21.2
RARA
p242
HOX2
NGFR
1.4
D17S80
PPY
5.0
D17S509*
D17S52
3.0
D17S508
21.3
6.1
D17S507
NME1
MPO
D17S41
9.7
D17S86*
D17S774
APOH
GH1
D17S497
D17S35
3.4
D17S504*
22
PRKCA
3.3
D17S40
D17S43
7.8
D17S503*
1.5
D17S515*
2.5
D17S21
23
D17S767
7.3
D17S20
TK1
D17S500
4.1
D17S4
D17S764
3.3
D17S772
24
D17S773
3.9
D17S77
3.4
D17S501
1.6
D17S502
D17S770
D17S768
D17S763*
D17S512*
5.4
D17S26*
25
4.6
D17S24*
D17S27
D17S765*
D17S766*
1.9
1.4
D17S79*
D17S775*

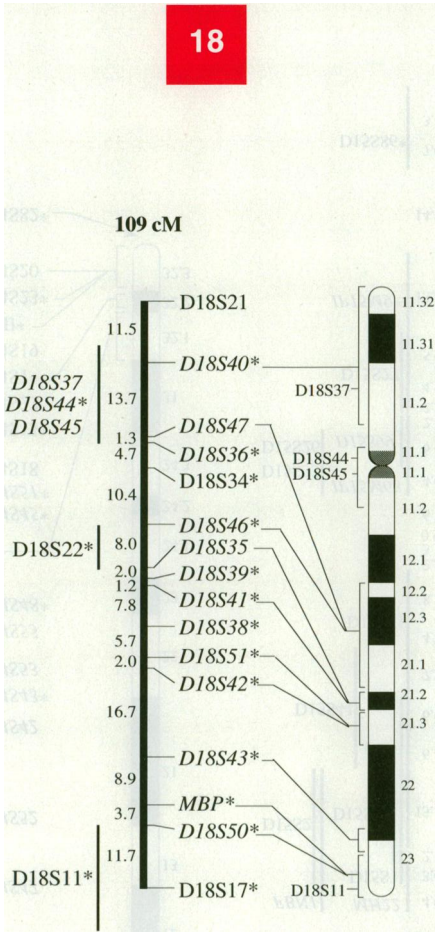
18
109 cM
D18S21
11.5
D18S40*
D18S37
D18S44*
D18S45
13.7
D18S47
1.3
D18S36*
4.7
D18S34*
10.4
D18S46*
D18S22*
8.0
D18S35
2.0
D18S39*
1.2
D18S41*
7.8
D18S38*
5.7
D18S51*
2.0
D18S42*
16.7
D18S43*
8.9
MBP*
3.7
D18S50*
11.7
D18S11*
D18S17*
11.32
11.31
11.2
D18S37
11.1
D18S44
D18S45
11.1
11.2
12.1
12.2
12.3
21.1
21.2
21.3
22
23
D18S11

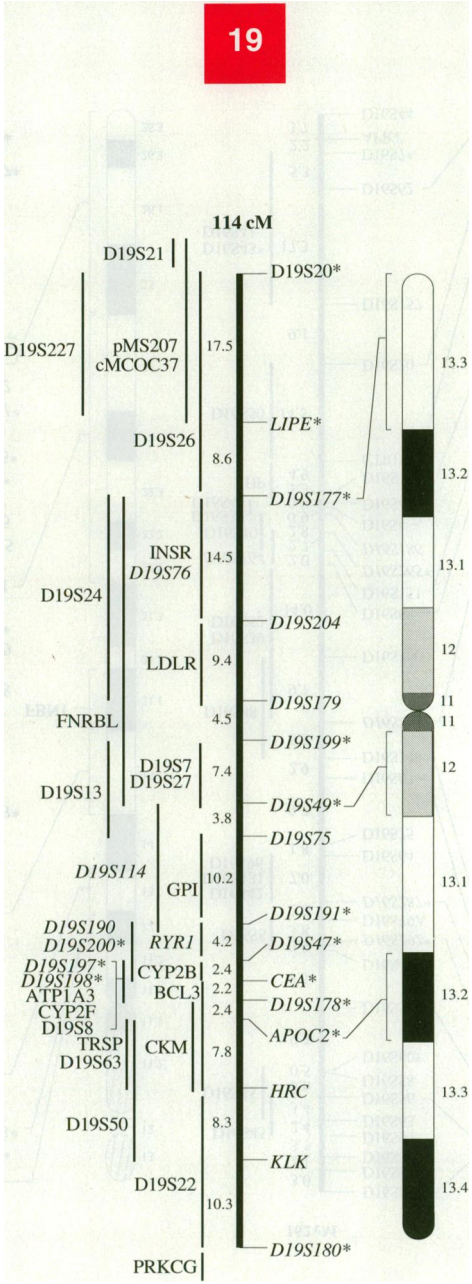
19
114 cM
D19S21
D19S20*
D19S227
pMS207
cMCOC37
17.5
13.3
LIPE*
D19S26
8.6
13.2
D19S177*
INSR
D19S76
14.5
13.1
D19S24
D19S204
LDLR
9.4
12
D19S179
11
FNRBL
4.5
11
D19S199*
D19S7
D19S27
7.4
12
D19S13
D19S49*
3.8
D19S75
D19S114
GPI
10.2
13.1
D19S191*
D19S190
D19S200*
RYR1
4.2
D19S47*
D19S197*
D19S198*
CYP2B
2.4
CEA*
ATP1A3
BCL3
2.2
13.2
D19S178*
CYP2F
2.4
D19S8
APOC2*
TRSP
D19S63
CKM
7.8
HRC
13.3
D19S50
8.3
KLK
D19S22
10.3
13.4
PRKCG
D19S180*

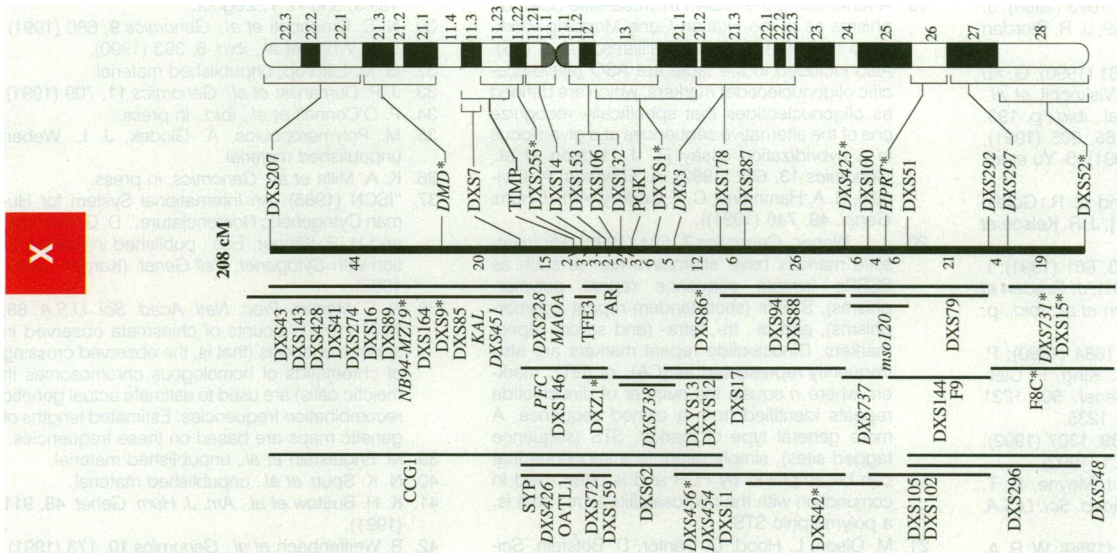
X
208 cM
DXS207
DMD*
DXS7
TIMP
DXS255*
DXS14
DXS153
DXS106
DXS132
PGK1
DXYS1*
DXS3
DXS178
DXS287
DXS425*
DXS100
HPRT*
DXS51
DXS292
DXS297
DXS52*
DXS43
DXS143
DXS428
DXS41
DXS274
DXS16
DXS89
NB94-MZ19*
DXS164
DXS9*
DXS85
KAL
DXS451
DXS228
MAOA
TFE3
AR
DXS86*
DXS94
DXS88
mso120
DXS79
DXS731*
DXS15*
PFC
DXS146
DXZ1*
DXS738
DXYS13
DXYS12
DXS17
DXS737
DXS144
F9
F8C*
CCG1
SYP
DXS426
OATL1
DXS72
DXS159
DXS62
DXS456*
DXS454
DXS11
DXS42*
DXS105
DXS102
DXS296
DXS548

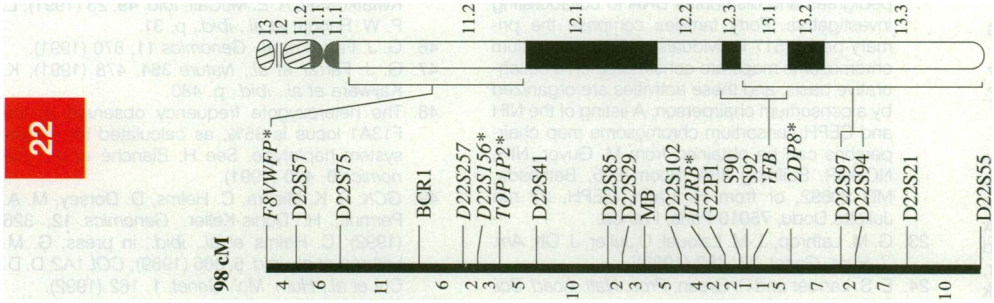
22
98 cM
F8VWFP*
D22S57
D22S75
BCR1
D22S257
D22S156*
TOP1P2*
D22S41
D22S85
D22S29
MB
D22S102
IL2RB*
G22P1
S90
S92
iFB
2DP8*
D22S97
D22S94
D22S21
D22S55

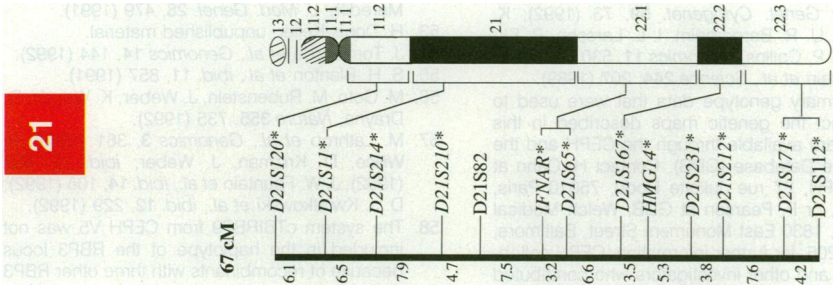
21
67 cM
D21S120*
D21S11*
D21S214*
D21S210*
D21S82
IFNAR*
D21S65*
D21S167*
HMG14*
D21S231*
D21S212*
D21S171*
D21S112*

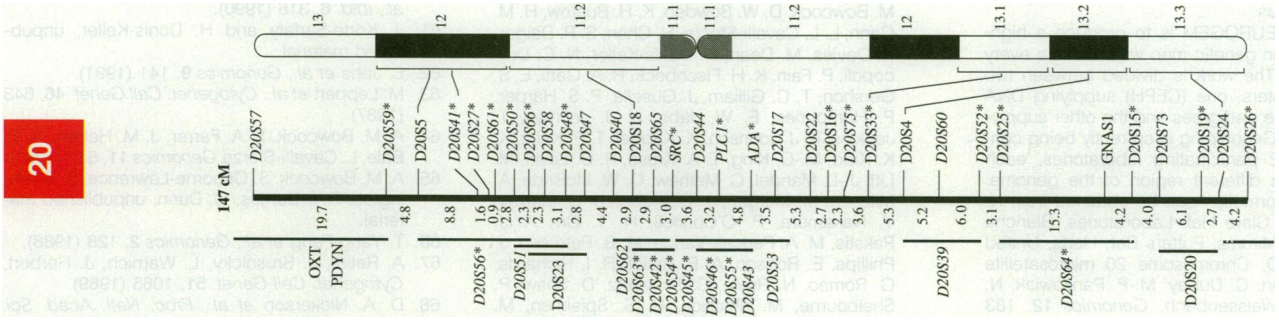
20
147 cM
D20S57
D20S59*
D20S5
D20S41*
D20S27*
D20S61*
D20S50*
D20S66*
D20S58
D20S48*
D20S47
D20S40
D20S18
D20S65
SRC*
D20S44
PLC1*
ADA*
D20S17
D20S22
D20S16*
D20S75*
D20S33*
D20S4
D20S60
D20S52*
D20S25*
GNAS1
D20S15*
D20S73
D20S19*
D20S24
D20S26*
OXT
PDYN
D20S56*
D20S51
D20S23
D20S62
D20S63*
D20S42*
D20S54*
D20S45*
D20S46*
D20S55*
D20S43
D20S53
D20S39
D20S64*
D20S20

REFERENCES AND NOTES

1. B. S. Kerem *et al.*, *Science* **245**, 1073 (1989); J. M. Rommens *et al.*, *ibid.*, p. 1059; J. R. Riordan *et al.*, *ibid.*, p. 1066.
2. M. R. Wallace *et al.*, *ibid.* **249**, 181 (1990); G. Xu *et al.*, *Cell* **62**, 599 (1990); D. Viskochil *et al.*, *ibid.*, p. 187; R. M. Cawthon *et al.*, *ibid.*, p. 193.
3. A. J. M. H. Verkek *et al.*, *Cell* **65**, 905 (1991); Y.-H. Fu *et al.*, *ibid.* **67**, 1047 (1991); S. Yu *et al.*, *Science* **252**, 1179 (1991).
4. Reviewed by E. S. Gershon and L. R. Goldin [*Genet. Epidemiol.* **6**, 201 (1989)]; J. R. Kelsoe *et al.*, *Nature* **342**, 238 (1989).
5. K. W. Kinzler *et al.*, *Science* **253**, 661 (1991); I. Nishisho *et al.*, *ibid.*, p. 665 (1991); J. Groden *et al.*, *Cell* **66**, 589 (1991); G. Joslyn *et al.*, *ibid.*, p. 601.
6. J. M. Hall *et al.*, *Science* **250**, 1684 (1990); P. Margaritte, Bonautu-Pellie, M-C. King, F. Clerget-Darpoux, *Am. J. Hum. Genet.* **50**, 1231 (1992); J. M. Hall *et al.*, *ibid.*, p. 1235.
7. A. T. Hattersley *et al.*, *Lancet* **339**, 1307 (1992); N. Vionnet *et al.*, *Nature* **356**, 721 (1992).
8. H. C. Riethman, R. K. Moyzis, J. Meyne, D. T. Burke, M. V. Olson, *Proc. Natl. Acad. Sci. U.S.A.* **86**, 6240 (1989).
9. W. R. A. Brown, *Nature* **338**, 774 (1989); W. R. A. Brown *et al.*, *Cell* **63**, 119 (1990).
10. A. O. M. Wilkie *et al.*, *Cell* **64**, 595 (1991).
11. D. Botstein, R. L. White, M. Skolnick, R. W. Davis, *Am. J. Hum. Genet.* **32**, 314 (1980).
12. H. Donis-Keller *et al.*, *Cell* **51**, 319 (1987).
13. Y. Nakamura *et al.*, *Science* **235**, 1616 (1987); G. Vergnaud *et al.*, *Genomics* **11**, 135 (1991).
14. J. A. L. Armour *et al.*, *Nucleic Acids Res.* **17**, 4925 (1989); N. J. Royle, R. E. Clarkson, Z. Wong, A. J. Jeffreys, *Genomics* **3**, 352 (1988).
15. Y. Nakamura *et al.*, *ibid.* **4**, 76 (1989).
16. The "index map" project was initiated in April 1991 and is scheduled for completion in mid-1993. Other criteria for "index markers" are ease of use and preference for assay by PCR. Index markers will comprise the maps, which should therefore be termed "index maps"; however, they have also been referred to as "framework maps," which is somewhat confusing because the same term has been applied previously to maps for which only the unambiguous ordering of markers was considered important (that is, the informativeness of the marker and assay method is not taken into consideration) [B. J. B. Keats, S. L. Sherman, J. Ott, *Cytogenet. Cell Genet.* **58**, 1097 (1991)]. Other map categories reflect marker definitions. For example, "reference markers" fulfill the criteria of unambiguous placement on a linear map and are useful for physical and genetic mapping; they would be designated by consensus as the "best marker available for a given interval" [R. Williamson *et al.*, *Cytogenet. Cell Genet.* **58**, 1190 (1991)]. A genetic locus may be defined as continuous DNA sequence at a specific position on a chromosome; it may be a gene or an "anonymous" sequence (typically a sequence contained in a clone of several kilobases in size). Inheritance of mutations within the sequence at a locus define allele systems. One locus can be mapped genetically by using one or more systems found at the same locus.
17. The goal of EUROGEM is to produce a high-density human genetic map with markers every 5 to 10 cM. The work is divided between two resource centers, one (CEPH) supplying DNA from reference pedigrees and the other supplying markers. Genotyping is currently being conducted in 22 participating laboratories, each working on a different region of the genome. Additional information can be obtained from N. Spurr, ICRF, Clare Hall Laboratories, Blanche Lane, South Mimms, Potters Bar, Herts, United Kingdom 3LD. Chromosome 20 microsatellite map: J. Hazan, C. Dubay, M.-P. Pankowiak, N. Becuwe, J. Weissenbach, *Genomics* **12**, 183 (1992).
18. J. L. Weber and P. E. May, *Am. J. Hum. Genet.* **44**, 388 (1989); M. Litt and J. A. Luty, *ibid.*, p. 397.
19. A table listing the known microsatellite polymorphisms as of the Human Gene Mapping Workshop 11 (1991) is given in Williamson *et al.* (*16*). Also included in the table are ASO (allele-specific oligonucleotide) markers, which are defined as oligonucleotides that specifically recognize one of the alternative sequences at a given locus in a hybridization assay [T. J. Hudson *et al.*, *Genomics* **13**, 622 (1992); A. Edwards, A. Civitello, H. A. Hammond, C. T. Caskey, *Am. J. Hum. Genet.* **49**, 746 (1991)].
20. J. L. Weber, *Genomics* **7**, 524 (1990). Microsatellite markers have alternative names such as SSRPs (simple sequence repeat polymorphisms), STRPs (short tandem repeat polymorphisms), and di-, tri-, tetra- (and so on) repeat markers. Dinucleotide repeat markers are also frequently represented as $(CA)_n$ or $(GT)_n$ markers where n equals the number of dinucleotide repeats identified from a cloned sequence. A more general type of marker, STS (sequence tagged sites), simply refers to a sequence that can be amplified by PCR and is often used in conjunction with the microsatellite term—that is, a polymorphic STS.
21. M. Olson, L. Hood, C. Cantor, D. Botstein, *Science* **245**, 1434 (1989).
22. J. Dausset, *Genomics* **6**, 575 (1990). The CEPH maintains a set of lymphoblastoid cell lines from a panel of mainly three-generation reference pedigrees and distributes DNA to collaborating investigators. Forty families comprise the primary panel (517 individuals). CEPH consortium chromosome maps are constructed on a collaborative basis, and these activities are organized by a consortium chairperson. A listing of the NIH and CEPH consortium chromosome map chairpersons can be obtained from M. Guyer, NIH, NCHGR, Building 38A, Room 605, Bethesda, MD 20892, or from H. Cann, CEPH, 27 rue Juliette Dodu, 75010 Paris, France.
23. G. M. Lathrop, J.-M. Lalouel, C Julier, J. Ott, *Am. J. Hum. Genet.* **37**, 482 (1985).
24. E. S. Lander and P. Green, *Proc. Natl. Acad. Sci. U.S.A.* **84**, 2363 (1987).
25. P. Green, CRI-MAP program package V2.4, unpublished material.
26. E. S. Lander *et al.*, *Genomics* **1**, 174 (1987).
27. I. Bieche *et al.*, *Lancet* **339**, 139 (1992).
28. P. Osella, A. Carlson, H. Wyandt, A. Milunsky, *Cancer Genet. Cytogenet.* **59**, 73 (1992); K. Kunimi, U. R. Bergerheim, I.-L. Larsson, P. Ekman, V. P. Collins, *Genomics* **11**, 530 (1991); B. Vogelstein *et al.*, *Science* **244**, 207 (1989).
29. The primary genotype data that were used to construct the genetic maps described in this report are available through the CEPH and the Genome Database (GDB). Contact H. Cann at the CEPH, 27 rue Juliette Dodu, 75010 Paris, France, or P. Pearson at GDB, Welch Medical Library, 1830 East Monument Street, Baltimore, MD 21205, for further information. CEPH collaborators and other investigators who contributed genotype data to the CEPH database used in the construction of the genetic linkage maps reported here are S. E. Antonarakis, I. Balazs, A. E. Bale, D. F. Barker, P. E. Barker, A. L. Beaudet, A. M. Bowcock, D. W. Bowden, K. H. Buetow, H. M. Cann, L. L. Cavalli-Sforza, H. Chen, S. P. Daiger, K. Davies, M. Dean, H. Donis-Keller, N. C. Dracopoli, P. Fain, K. H. Fischbeck, R. A. Gatti, E. S. Gershon, T. C. Gilliam, J. Gusella, P. S. Harper, P. Humphries, E. W. Jabs, A. J. Jeffreys, T. Jenkins, K. J. Johnson, K. Kappel, T. P. Keith, K. K. Kidd, M.-C. King, T. A. Kruse, R. C. Levitt, M. Litt, J.-L. Mandel, C. Mathew, O. W. McBride, A. Mitchell, M. Morgan, J. C. Mulley, J. C. Murray, Y. Nakamura, P. O'Connell, H. T. Orr, A. J. Pakstis, M. A. Pericak-Vance, M. B. Petersen, J. Phillips, E. Robson, A. E. Retief, R. I. Richards, G. Romeo, N. Royle, C. Schwartz, D. Shaw, P. Shelbourne, M. Skolnick, R. S. Spielman, M. Stephenson, G. R. Sutherland, P. Tsipouras, S. Rundle, G. Vergnaud, A. C. Warren, J. L. Weber, B. Weiffenbach, J. Weissenbach, R. L. White, P. J. Wilkie, H. F. Willard, R. Williamson, S. Wood, J. Yates, and H. Y. Zoghbi.
30. N. C. Dracopoli *et al.*, *Genomics* **9**, 686 (1991).
31. R. L. White *et al.*, *ibid.* **6**, 393 (1990).
32. G. M. Lathrop, unpublished material.
33. J. P. Dumanski *et al.*, *Genomics* **11**, 709 (1991).
34. P. O'Connell *et al.*, *ibid.*, in press.
35. M. Polymeropoulos, A. Glodek, J. L. Weber, unpublished material.
36. K. A. Mills *et al.*, *Genomics*, in press.
37. "ISCN (1985): An International System for Human Cytogenetic Nomenclature," D. G. Harnden and H. P. Klinger, Eds.; published in collaboration with *Cytogenet. Cell Genet.* (Karger, Basel, 1985).
38. N. E. Morton, *Proc. Natl. Acad. Sci. U.S.A.* **88**, 7474 (1991). Counts of chiasmata observed in spermatogenesis (that is, the observed crossing of chromatids of homologous chromosomes in meiotic cells) are used to estimate actual genetic recombination frequencies. Estimated lengths of genetic maps are based on these frequencies.
39. M. Engelstein *et al.*, unpublished material.
40. N. K. Spurr *et al.*, unpublished material.
41. K. H. Buetow *et al.*, *Am. J. Hum. Genet.* **48**, 911 (1991).
42. B. Weiffenbach *et al.*, *Genomics* **10**, 173 (1991).
43. M. Leppert *et al.*, *Science* **238**, 1411 (1987).
44. Y. Nakamura *et al.*, *Am. J. Hum. Genet.* **43**, 638 (1988).
45. H. Y. Zoghbi, C. Jodice, L. A. Sandkuijl, T. J. Kwiatkowski, A. E. McCall, *ibid.* **49**, 23 (1991); L. P. W. Ranum *et al.*, *ibid.*, p. 31.
46. G. J. Farrar *et al.*, *Genomics* **11**, 870 (1991).
47. G. J. Farrar *et al.*, *Nature* **354**, 478 (1991); K. Kajiwara *et al.*, *ibid.*, p. 480.
48. The heterozygote frequency observed at the F13A1 locus is 85%, as calculated for a four-system haplotype. See H. Blanché *et al.*, *Genomics* **9**, 420 (1991).
49. *GCK*: S. K. Mishra, C. Helms, D. Dorsey, M. A. Permutt, H. Donis-Keller, *Genomics* **12**, 326 (1992); C. Helms *et al.*, *ibid.*, in press; G. M. Lathrop *et al.*, *ibid.* **5**, 866 (1989); *COL1A2*: D. D. Chi *et al.*, *Hum. Mol. Genet.* **1**, 162 (1992).
50. B. Richards, C. Reeves, G. T. Horn, *Nucleic Acids Res.* **19**, 5798 (1991).
51. A. G. Hatziioannou, C. M. Krauss, M. B. Lewis, T. D. Halazonetis, *Am. J. Med. Genet.* **40**, 201 (1991).
52. S. H. Roberts, H. E. Hughes, S. J. Davies, A. L. Meredith, *J. Med. Genet.* **28**, 479 (1991).
53. H. Donis-Keller, unpublished material.
54. J. Tomfohrde *et al.*, *Genomics* **14**, 144 (1992).
55. S. H. Blanton *et al.*, *ibid.* **11**, 857 (1991).
56. M. Goto, M. Rubenstein, J. Weber, K. Woods, D. Drayna, *Nature* **355**, 735 (1992).
57. M. Lathrop *et al.*, *Genomics* **3**, 361 (1988); P. Wilkie, D. Krizman, J. Weber, *ibid.* **12**, 607 (1992); J. W. Fountain *et al.*, *ibid.* **14**, 105 (1992); D. J. Kwiatkowski *et al.*, *ibid.* **12**, 229 (1992).
58. The system cTBIRBP9 from CEPH V5 was not included in the haplotype of the RBP3 locus because of recombinants with three other RBP3 systems.
59. J. R. Howe *et al.*, *Am. J. Hum. Genet.*, in press.
60. R. White *et al.*, *Nature* **313**, 101 (1985); C. Julier *et al.*, *Genomics* **7**, 335 (1990); P. Charmley *et al.*, *ibid.* **6**, 316 (1990).
61. J. Korte-Sarfaty and H. Donis-Keller, unpublished material.
62. E. Jabs *et al.*, *Genomics* **9**, 141 (1991).
63. M. Leppert *et al.*, *Cytogenet. Cell Genet.* **46**, 648 (1987).
64. A. M. Bowcock, L. A. Farrer, J. M. Hebert, A. E. Bale, L. Cavalli-Sforza *Genomics* **11**, 517 (1991).
65. A. M. Bowcock, S. Osborne-Lawrence, S. Washington, R. I. Barnes, G. Dunn, unpublished material.
66. T. Yang-Feng *et al.*, *Genomics* **2**, 128 (1988).
67. A. Retief, J. Brusnicky, L. Warnich, J. Herbert, *Cytogenet. Cell Genet.* **51**, 1065 (1989).
68. D. A. Nickerson *et al.*, *Proc. Natl. Acad. Sci. U.S.A.* **87**, 8923 (1990); D. A. Nickerson *et al.*, *Genomics* **12**, 377 (1992).

69. Z. Wang and J. L. Weber, *Genomics* **13**, 532 (1992).
70. J. A. Jarcho *et al.*, *N. Engl. J. Med.* **321**, 1372 (1989); A. A. T. Geisterfer-Lowrance *et al.*, *Cell* **62**, 999 (1990); G. Tanigawa *et al.*, *ibid.*, p. 991.
71. Y. Nakamura *et al.*, *Genomics* **3**, 342 (1988).
72. A. M. Bowcock *et al.*, *ibid.*, in press.
73. D. F. Callen *et al.*, *ibid.* **13**, 1178 (1992).
74. P. Harris, unpublished material.
75. J. L. Weber, A. E. Kwitek, P. E. May, *Nucleic Acids Res.* **18**, 4034 (1990); A. D. Thompson *et al.*, *Genomics* **13**, 402 (1992).
76. C. Julier *et al.*, *Genomics* **6**, 419 (1990); T. P. Keith *et al.*, *Proc. Natl. Acad. Sci. U.S.A.* **87**, 5754 (1990).
77. R. L. Stallings *et al.*, *Genomics* **13**, 1031 (1992).
78. Y. Nakamura *et al.*, *ibid.* **2**, 302 (1988).
79. All microsatellites can be amplified as follows: at 94°C for 3 min, 26 cycles at 94°C 1 min, 55°C for 2 min, 72°C for 1 min, and a final extension of 72°C for 6 min.
80. B. J. B. Keats *et al.*, *Genomics* **9**, 557 (1991).
81. G. M. Lathrop, J. M Lalouel, C. Jalier, J. Ott, *Proc. Natl. Acad. Sci. U.S.A.* **81**, 3443 (1984).
82. R. E. Straub *et al.*, *Genomics*, in press.
83. P. O'Connell *et al.*, *ibid.* **3**, 367 (1988).
84. Y. Nakamura *et al.*, *ibid.*, p. 67; H. G. Brunner *et al.*, *ibid.* **5**, 589 (1989); T. V. McCarthy *et al.*, *Nature* **343**, 562 (1990); R. I. Richards *et al.*, *Genomics* **11**, 77 (1991); H. H. Ropers and M. A. Pericak-Vance, *Cytogenet. Cell Genet.* **58**, 751 (1991).
85. Y. Nakamura *et al.*, *Genomics* **5**, 945 (1989).
86. R. Williamson *et al.*, Cytogenet. Cell Genet. **58**, 1190 (1991).
87. M. G. McInnis *et al.*, unpublished material.
88. R. E. Tanzi *et al.*, *Genomics* **3**, 129 (1988); R. E. Tanzi *et al.*, *Am. J. Hum. Genet.* **50**, 551 (1992); A. C. Warren, S. A. Slaugenhaupt, J. G. Lewis, A. Chakravarti, S. E. Antonarakis, *Genomics* **4**, 579 (1989); M. B. Petersen *et al.*, *ibid.* **9**, 407 (1991).
89. G. A. Rouleau *et al.*, *Genomics* **4**, 1 (1989).
90. The HET, PIC, and NIM values for the X chromosome markers were calculated from a data set in which all hemizygous males were made to appear heterozygous in order for the linkage analysis programs to operate. This resulted in inflated values because a dummy allele with a frequency of approximately 0.25 was added to all systems and because all males with information will appear informative—that is, falsely heterozygous—and be counted in the NIM. The high HET values are calculated from the number of heterozygotes observed (from a small number of individuals in many cases), and normally a two-allele system would never exceed a PIC of 0.375.
91. D. Drayna *et al.*, *Proc. Natl. Acad. Sci. U.S.A.* **81**, 2836 (1984).
92. A. Poustka *et al.*, *ibid.* **88**, 8302 (1991).
93. Genome Database (GDB), Welch Medical Library, 1830 East Monument Street, Baltimore, MD 21205.
94. D. Page *et al.*, *Genomics* **1**, 243 (1987).
95. C. Petit, J. Levilliers, J. Weissenbach, *EMBO J.* **7**, 2369 (1988).
96. The first such map of approximately 30 Mb from the Y chromosome has been constructed [D. Vollrath *et al.*, *Science* **258**, 52 (1992); S. Foote *et al.*, *ibid.*, p. 60], and large segments of chromosome 21 and the X chromosome have also been assembled [S. Antonarakis, unpublished material; R. D. Little, G. Pilia, S. Johnson, M. D'Urso, D. Schlessinger, *Proc. Natl. Acad. Sci. U.S.A.* **89**, 177 (1992)].
97. H. F. Willard and J. S. Waye, *Trends Genet.* **3**, 192 (1988); G. M. Greig and H. F. Willard, *Genomics* **12**, 573 (1992); G. Vissel and K. H. Choo, *Nucleic Acids Res.* **19**, 271 (1991).
98. M. A. Permutt, unpublished material.
99. K. H. Buetow, *Am. J. Hum. Genet.* **49**, 985 (1991).
100. For RFLP markers, retyping may not be practical because the markers are not always available and the assay technology is rapidly becoming outmoded. In the case of microsatellite markers, it is relatively easy to retype the markers. However, electronic transmission of primary data as image files to laboratories remote from the site originating the data could greatly improve the efficiency of error checking and make previously generated RFLP data more useful. Such efforts to improve communications of this type are under way in several laboratories [P. Cartwright and H. Donis-Keller, unpublished material; H. A. Drury *et al.*, *BioTechniques* **12**, 892 (1992)]. As clone-based maps are expanded to cover Mb regions, ambiguities of genetic marker order should be clarified. Similarly, ambiguities regarding continuity of clone-based maps along chromosomes may be solved by genetic mapping information.
101. Cell lines for 21 CEPH families are currently available from the NIGMS Mutant Cell Repository, Coriell Institute, Camden, NJ.
102. The complete 315-kb sequence of yeast chromosome III has been reported, uniting genetic and physical information [S. G. Oliver *et al.*, *Nature* **357**, 38 (1992)].
103. The map graphics were assembled with the aid of a computer program, Vertical Mapper (Six Ponds Software), written for the Macintosh.

104. We acknowledge the ongoing support and involvement of J. Dausset and the staff of the Centre d'Étude du Polymorphisme Humain (CEPH), which since 1984 has provided DNA from reference families and a database of genotypes to the laboratories represented in this publication.
105. We thank the following members of the Donis-Keller laboratory for preparing the map graphics and tables, for assisting with error checking of the data as presented, and for project coordination: C. Helms, T. Steinbrueck, R. Normington, L. Liu, S. Steinbrueck, R. Weaver, T. Repko, and M. Akin. This work was supported in part by NIH grants HG00373 and HD24605 (S.E.A.), HG00461 (A.M.B.), DK41269 (D.W.B.), HG00425 (K.H.B.), HG00774 (A.C.), HG00395 (N.C.D.), HG00469 (H.D.-K.), HG00462 (T.C.G.), HG00319 (J.F.G.), HG00324 (J.L.H.), HG00460 (T.P.K.), HG00365 and NIMH MH39239 (K.K.K.), HG00598 (D.J.K.), HG00022 (M.L.), HG00355 and HG00206 (J.C.M. and K.H.B.), HG00490 (S.L.N. and H.A.D.), HG00470 (S.L.N. and S.L.S.), HG00464 (D.A.N.), CA55772 and HG00470 (P.O'C.), HG00167 and HG00164 (J.O.), DK35592 (J.P.), NS26630 (M.A.P.-V.), HG00073 (S.S.), HG00248 (J.L.W.), HG00367 (R.L.W. and J.-M.L.), NS27699 (H.Y.Z.); by the Howard Hughes Medical Institute (R.L.W. and J.-M.L.); and by grants from the Coles Family Foundation (P.T.), the Department of Energy, FG02-88ER606889 (D.F.B. and P.R.F.), the Medical Research Council as part of the United Kingdom Human Genome Mapping Project and Eurogem (S.P. and M.F.-S.), National Health and the Medical Research Council of Australia (G.R.S.), NSF DIR8809710 (L.H.), the State of South Carolina Mental Health Department (C.S.), and the Wellcome Trust (J.A.). Addresses of authors listed in chromosome order:

Chromosome 1: [a]Dept. of Biology, Massachusetts Institute of Technology, Cambridge, MA 02139; [b]Dept. of Pathology, University of Texas Health Science Center at San Antonio, San Antonio, TX 78284; [c]Howard Hughes Medical Institute and Dept. of Human Genetics, University of Utah Medical Center, Salt Lake City, UT 84132; [d]Fox Chase Center, Philadelphia, PA 19111; [e]Dept. of Pediatrics, University of Iowa, Iowa City, IA 52242; [f]Div. of Human Molecular Genetics, Dept. of Surgery, Washington University School of Medicine, St. Louis, MO 63110; [g]School of Public Health, University of California, Berkeley, CA 94720; [h]The Galton Laboratory, University College London, London NW1 2HE, United Kingdom; [i]Dept. of Community Medicine, University of Southampton, Southampton S09 4XY, United Kingdom; [j]Dept. of Genetics, Stanford University School of Medicine, Stanford, CA 94305; [k]Dept. of Genetics, University of Leicester, Leicester LE1 7RH, United Kingdom; [l]MRC Human Ecogenetics Research Unit, Dept. of Human Genetics, South African Institute for Medical Research and University of Witwatersrand, Johannesburg 2000, South Africa; [m]Marshfield Medical Research Foundation, Marshfield, WI 54449; [n]Dept. of Human Genetics, Yale University School of Medicine, New Haven, CT 6510.

Chromosome 2: [a]Div. of Human Molecular Genetics, Dept. of Surgery, Washington University School of Medicine, St. Louis, MO 63110; [b]Marshfield Medical Research Foundation, Marshfield, WI 54449.

Chromosome 3: [a]Dept. of Cellular and Structural Biology, University of Texas Health Science Center, San Antonio, TX 78284; [b]Div. of Medical Genetics, Emory University, Atlanta, GA 30322; [c]Div. of Medical Oncology, Eleanor Roosevelt Institute, Denver, CO 80206; [d]Dept. of Molecular Genetics, Marshfield Medical School, Marshfield, WI 54449; [e]Div. of Biochemistry, Cancer Institute, Toshima-ku, Tokyo 170, Japan.

Chromosome 4: [a]Dept. of Pediatrics, University of Iowa, Iowa City, IA 52242; [b]Div. of Population Science, Fox Chase Cancer Center, Philadelphia, PA 19111; [c]Massachusetts Institute of Technology, Cambridge, MA 02139; [d]Marshfield Medical Research Foundation, Marshfield, WI 54449.

Chromosome 5: [a]Dept. of Human Genetics, University of Utah, and Eccles Institute of Human Genetics, Salt Lake City, UT 84112; [b]Dept. of Psychiatry, University of Utah Medical School, Salt Lake City, UT 84132; [c]Dept. of Medical Genetics, University of British Columbia, Vancouver, British Columbia V6T 1Z3, Canada; [d]Dept. of Genetics, University of Leicester, Leicester LE1 7RH, United Kingdom; [e]Div. of Biochemistry, Cancer Institute, Toshima-ku, Tokyo 170, Japan; [f]Dept. of Genetics, University of Stellenbosch, Stellenbosch 7600, South Africa; [g]Dept. of Human Genetics and Molecular Biology, Collaborative Research, Inc., Waltham, MA 02154; [h]Howard University Medical Institute, University of Utah, and Eccles Institute of Human Genetics, Salt Lake City, UT 84112.

Chromosome 6: [a]Div. of Human Molecular Genetics, Dept. of Surgery, Washington University School of Medicine, St. Louis, MO 63110; [b]Dept. of Pediatrics and Institute of Molecular Genetics, Baylor College of Medicine, Houston, TX 77030; [c]Institute of Human Genetics, University of Minnesota, Minneapolis, MN 55455; [d]Centre d'Étude du Polymorphisme Humain (CEPH), Paris 75010, France.

Chromosome 7: [a]Div. of Human Molecular Genetics, Dept. of Surgery, Washington University School of Medicine, St. Louis, MO 63110; [b]Centre d'Etudes du Bouchet, 91710 Vert le Petit, France.

Chromosome 8: [a]Div. of Human Molecular Genetics, Dept. of Surgery, Washington University School of Medicine, St. Louis, MO 63110; [b]Graduate School of Biomedical Sciences, University of Texas Health Science Center, Houston, TX 77030; [c]Marshfield Medical Institute, Marshfield, WI 54449; [d]Dept. of Medical Genetics, University of British Columbia, Vancouver, British Columbia V6T 1Z3, Canada.

Chromosome 9: [a]Dept. of Medicine, Brigham and Women's Hospital, Harvard Medical School, Boston, MA 02115; [b]MRC Human Biochemical Genetics Unit, University College London, London NW1 2HE, United Kingdom; [c]Dept. of Genetics, University of Leicester, Leicester LE1 7RH, United Kingdom; [d]Dept. of Pathology, Camridge University, Cambridge CB2 1QP, United Kingdom; [e]Molecular Neurogenetics Laboratory, Massachusetts General Hospital, Harvard Medical School, Boston, MA 02115; [f]Div. of Neurology, Duke University Medical Center, Durham, NC 27710; [g]Centre d'Etudes du Bouchet, 91710 Vert le Petit, France; [h]Dept. of Genetics, University of Stellenbosch, Stellenbosch 7600, South Africa.

Chromosome 10: [a]Dept. of Human Genetics

and Molecular Biology, Collaborative Research, Inc., Waltham, MA 02154; [b]CEPH, 75010 Paris, France; [c]Marshfield Medical Resaerch Foundation, Marshfield, WI 54449; [d]Centre d'Etudes du Bouchet, 91710 Vert le Petit, France.

Chromosome 11: Depts. of [a]Molecular and Medical Genetics, [b]Neurology, and [e]Biochemistry and Molecular Biology, Oregon Health Sciences University, Portland, OR 97201; [c]Marshfield Medical Research Foundation, Marshfield, WI 54449, [d]CEPH, Paris 75010, France.

Chromosome 12: [a]Div. of Human Molecular Genetics, Dept. of Surgery, Washington University School of Medicine, St. Louis, MO 63110; [b]Marshfield Medical Research Foundation, Marshfield, WI 54449.

Chromosome 13: [a]Dept. of Pediatrics, University of Texas Southwestern Medical Center, 5323 Dallas, TX 75235; [b]Howard Hughes Medical Institute and Dept. of Human Genetics, University of Utah Medical Center, Salt Lake City, UT 84132; [c]Centre d'Etudes du Bouchet, 91710 Vert le Petit, France; [d]Dept. of Genetics, University of Stellenbosch, Stellenbosch 7600, South Africa.

Chromosome 14: [a]Div. of Human Molecular Genetics, Dept. of Surgery, Washington University School of Medicine, St. Louis, MO 63110; [b]Marshfield Medical Research Foundation, Marshfield, WI 54449; [c]Depts. of Molecular and Medical Genetics and of Biochemistry and Molecular Biology, Oregon Health Sciences University, Portland, OR 92701; [d]Dept. of Molecular Biology, University of Washington School of Medicine, Seattle, WA 98195.

Chromosome 15: [a]Dept. of Pediatrics, University of Texas Southwestern Medical Center, 5323 Dallas, TX 75235; [b]Dept. of Biology, Massachusetts Institute of Technology, Cambridge, MA 02139; [c]Dept. of Pediatrics, The University of Connecticut Health Center, Farmington, CT 06030; [d]MRC Human Ecogenetics Research Unit, Dept. of Human Genetics, School of Pathology, South African Institute for Medical Research, and the University of the Witwatersrand, Johannesburg 2000, South Africa; [e]Centre d'Etudes du Bouchet, 91710 Vert le Petit, France.

Chromosome 16: Dept. of Cytogenetics and Molecular Genetics, Adelaide Children's Hospital, North Adelaide, South Australia, Australia 5006.

Chromosome 17: [a]Dept. of Pathology, University of Texas Health Science Center at San Antonio, San Antonio, TX 78284; Depts. of [b]Psychiatry and of [c]Genetic Epidemiology, University of Utah, Salt Lake City, UT 84108; [d]Dept. of Human Genetics, Yale University School of Medicine, New Haven, CT 06510; [e]Genetics Division, Vanderbilt University Medical Center, Nashville, TN 37232; [f]Centre d'Etudes du Bouchet, 91710 Vert le Petit, France; [g]Greenwood Genetic Center, Greenwood, SC 29646; [h]Marshfield Medical Research Foundation, Marshfield, WI 54449; [i]Laboratory of Biochemistry, National Cancer Institute, National Institutes of Health, Bethesda, MD 20892; [j]Dept. of Genetics, Stanford University School of Medicine, Stanford, CA 94305; [k]Lifecodes Corp., Valhalla, NY 10595; [l]Div. of Medical Genetics, University of Iowa Hospitals, Iowa City, IA 52242; [m]Howard Hughes Medical Institute and Dept. of Human Genetics, University of Utah, Salt Lake City, UT 84112.

Chromosome 18: [a]Depts. of Psychiatry and of Genetics and Development, Columbia University, and New York State Psychiatric Institute, New York, NY 10032; [b]Dept. of Biochemistry and Molecular Biology, Thomas Jefferson University, Philadelphia, PA 19107; [c]Dept. of Pathology, University of Texas Health Sciences Center at San Antonio, San Antonio, TX 78284.

Chromosome 19: [a]Marshfield Medical Research Foundation, Marshfield, WI 54449; [b]Institute of Medical Genetics, University of Wales College of Medicine, Cardiff CF4 4XN, United Kingdom; [c]Dept. of Psychiatry, Columbia University, New York, NY 10032.

Chromosome 20: [a]Dept. of Human Genetics and Molecular Biology, Collaborative Research, Inc., Waltham, MA 02154; [b]Dept. of Biochemistry, Bowman Gray School of Medicine, Wake Forest University, Winston-Salem, NC 27157; [c]Marshfield Medical Research Foundation, Marsh- field, WI 54449; [d]Clinical Neurogenetics Branch, National Institute of Mental Health, Bethesda, MD 20892; [e]Unité de Genetique Moleculaire Humaine, CNRS URA 1445, and Institut Pasteur, 28 rue du Docteur Roux, Paris 75015, France.

Chromosome 21: [a]Center for Medical Genetics, Johns Hopkins University School of Medicine, Baltimore, MD 21205; [b]Dept. of Human Genetics, University of Pittsburgh, Pittsburgh, PA 15261; [c]Dept. of Biochemistry, Oregon Health Sciences University, Portland, OR 97201.

Chromosome 22: [a]Molecular Neurogenetics Laboratory, Massachusetts General Hospital, Charlestown, MA 02129; [b]Div. of Population Science, Fox Chase Cancer Center, Philadelphia, PA 19111.

Chromosome X: [a]Dept. of Pediatrics, University of Iowa, Iowa City, IA 52242; [b]Div. of Population Science, Fox Chase Center, Philadelphia, PA 19111.